arXiv:cond-mat/0210245v1 [cond-mat.soft] 10 Oct 2002

Where the linearized Poisson-Boltzmann cell model fails: (I) spurious phase separation in charged colloidal suspensions

M. N. Tamashiro and H. Schiessel
Max-Planck-Institut für Polymerforschung,
Ackermannweg 10, 55128 Mainz, Germany

Abstract

We perform a linearization of the Poisson-Boltzmann (PB) density functional for spherical Wigner-Seitz cells that yields Debye-Hückel-like equations agreeing asymptotically with the PB results in the weak-coupling (high-temperature) limit. Both the canonical (fixed number of microions) as well as the semi-grand-canonical (in contact with an infinite salt reservoir) cases are considered and discussed in a unified linearized framework. In the canonical case, for sufficiently large colloidal charges the linearized theory predicts the occurrence of a thermodynamical instability with an associated phase separation of the homogeneous suspension into dilute (gas) and dense (liquid) phases. In the semi-grand-canonical case it is predicted that the isothermal compressibility and the osmotic-pressure difference between the colloidal suspension and the salt reservoir become negative in the low-temperature, high-surface charge or infinite-dilution (of polyions) limits. As already pointed out in the literature for the latter case, these features are in disagreement with the exact nonlinear PB solution inside a Wigner-Seitz cell and are thus artifacts of the linearization. By using explicitly gauge-invariant forms of the electrostatic potential we show that these artifacts, although thermodynamically consistent with quadratic expansions of the nonlinear functional and osmotic pressure, may be traced back to the non-fulfillment of the underlying assumptions of the linearization.

1 Introduction

The study of classical charged systems has received an increased renewed interest in view of many industrial applications:[1,2] paint, petrochemicals, food, pharmaceuticals, cosmetics, diapers, sewage treatment etc. Many environmental-friendly new materials are hydrosoluble due to the presence of ionizable groups that dissociate upon contact with water. In fact, their hydrosolubility is a result of the combination of Coulomb repulsion between fixed charged monomers and the mixing entropy maximized by the mobility in solution of the oppositely-charged small counterions. Besides technological applications, charged macromolecules like lipid aggregates (bilayers, micelles and vesicles), proteins and polynucleotides (including DNA and RNA) are also of fundamental importance in the biochemistry of living systems.[3,4] Furthermore, due to the availability of faster computers, many new insights in soft-matter physics come from Monte-Carlo and molecular-dynamics simulations of charged systems.[5,6] These may be partially viewed as controlled theoretical experiments and provide a complementary approach to analytical treatments.

An ubiquitous case is that of mesoscopic charged colloidal particles (also called polyions or macroions) immersed in aqueous solution, which polarize the small mobile ions in their vicinity: microions of opposite sign (counterions) are attracted to them, while like-sign microions (coions) are repelled. The theoretical description of these systems requires the understanding of the role of the electrostatic interactions between charged objects mediated by the surrounding aqueous ionic solution. In view of the many-body problem and the long-range nature of the Coulomb interaction, a statistical-mechanical treatment of the system is nontrivial. Within the Primitive Model[7] (PM) the molecular nature of the solvent is ignored (neglect of van der Waals and hydration forces) and the suspension is treated as a two-component system, comprised of the highly-charged large polyions (and its neutralizing counterions) and oppositely-charged pairs (anions and cations) of ionized salt particles. These are immersed in a continuous medium of dielectric constant ϵ and interact through the bare Coulomb potential with additional hard-sphere repulsion. In the PM it is implicitly assumed that the (hard) spheres have the same dielectric constant as the solvent, so there are no electrostatic

image effects. For symmetric (in size and charge) electrolytes the PM reduces to the Restricted Primitive Model (RPM) and a theoretical description for dilute solutions may be developed using the traditional Debye-Hückel (DH) theory for electrolytes,[8,9,10] with some improvements taking nonlinearities[11] into account or using integral-equation methods.[10] An extension of these theories for a colloidal suspension is nontrivial[12,13] in view of the huge asymmetry between poly- and microions. Compared to the symmetric case, nonlinearities are magnified and dominate in the strong asymmetric colloidal limit.

A mean-field approach to the PM, although not thermodynamically consistent,[14,15] is represented by the Poisson-Boltzmann (PB) approximation.[16,17,19,18] This treatment gives a reasonable description in the weak-coupling (high temperature or small charge densities) limit, when the microionic correlations that are neglected at the mean-field level are unimportant. But even the mean-field PB approximation for a suspension of charged polyions is a formidable task[20] due to the large asymmetry in size, mass and charge between the polyions and the small mobile ions. To circumvent this problem, the cell model has been introduced — originally for the cylindrical geometry[21,22] — which reduces the many-body problem to the study of a (fixed) single polyion inside a Wigner-Seitz (WS) cell, whose volume is related to the polyion density. In the WS-cell model the single polyion plays only the role of a *boundary condition.* Note that this represents a dramatic simplification to the original PM formulation, where polyions and microions are treated at the same level. Even though the applicability of the WS-cell model appears at first sight to be only justified for an ordered crystalline phase, it has also been used to describe the fluid phase,[23,24] neglecting thus the polyion translational entropy, the polyion-polyion interactions and *intercell* (both microion-polyion and microion-microion) correlations — *intracell* microion-microion correlations are neglected because of the mean-field approximation, which computes only the *intracell* microion-polyion correlations. To simplify further, the geometry of the WS cell is usually taken as to match the boundary condition on the polyion charged surface. For example, for colloidal particles a spherical charged polyion is considered inside a concentric spherical WS cell. This reduces the problem to the solution of a second-order ordinary (rather than partial) differential equation. For the spherical geometry this requires the numerical solution of the nonlinear PB equation, contrary to the planar[25,26,27] and cylindrical[21,22,28] cases, when an exact analytical solution is possible. In analogy to the DH approach to the RPM, it would be thus very helpful to formulate a linearized version of the PB approximation for WS-cell models. We should remark, however, that the linearized version (at the mean-field level) of the WS-cell model does not include any *intercell* (neither polyion-microion nor microion-microion) correlations and *intracell* microion-microion correlations, contrary to the traditional DH approach to the (symmetric) RPM, which automatically includes them because in the RPM the mean-field contribution — which in the PB WS-cell model comes from the *intracell* polyion-microion correlations — vanishes.[15] Therefore a more appropriate interpretation of the linearized equations to be obtained here is that they correspond to an expansion about the weak-coupling or high-temperature limit of the mean-field equations.

However, expressions obtained within a linearized framework should be interpreted with caution, since they may lead to artifacts when applied outside their range of validity. Besides the specific case to be discussed in this paper, another example which is clearly an artifact of the linearization corresponds to the attractive component to the effective interaction between two confined colloids induced by charged walls, predicted under linearized theory[29] but in violation to the exact (at mean-field level) nonlinear PB repulsion.[30] Although earlier numerical analysis of the nonlinear solution were in agreement with the linearized theory,[31] these were soon ruled out under very general conditions.[30] The disagreement with the rigorous nonlinear results might be attributed to flaws in the numerical calculations. Attempts to include ionic correlations lead indeed to attractive contributions to the effective interaction,[32,33] but they are doubly-screened and thus are not able to overcome the repulsive electrostatic DLVO[34,35] (Derjaguin-Landau-Verwey-Overbeek) component. Therefore, experimental evidences of confinement-induced attraction[36,37,38] and the occurrence of metastable superheated crystals[39] can not be explained at the PB mean-field level and still remain an open question.[40]

Almost two decades after the first experimental evidences of attraction between like-charged spherical colloids mediated by monovalent counterions in bulk deionized aqueous suspensions, its existence is still under dispute. Under the mentioned conditions, electrostatic-stabilized colloidal crystals have been investigated by Ise *et al.*,[41] revealing the presence of empty regions (voids) inside the crystal. These experimental observations were interpreted as a coexistence between a dense crystalline phase and a dilute gas phase. Similar voids were also found experimentally in the fluid phase,[42] which, in analogy to the critical behaviour

of symmetric electrolytes, were interpreted as a coexistence between dilute (gas) and dense (liquid) fluid phases. Even fully equilibrated macroscopic gas-liquid phase separation has been reported,[43] although these experimental observations have been attributed to the presence of ionic impurities.[44]

From the theoretical point-of-view attractive interactions between like-charged spheres are observed only under special conditions. For example, they have been seen in Monte Carlo simulations in the presence of multivalent counterions[45,46,47] or when the low-temperature ordering of the discrete charges is taken into account.[48] Under the conditions described in the previous paragraph those controversial experimental findings are either attributed to the presence of long-range attractive electrostatic interactions between like-charged polyions[49] or by state-independent volume terms[50,51] obtained by approximations that involve some kind of linearization: random-phase approximation,[52,53,54] DH pair-distribution functions augmented by a variational approach for the polyion-polyion interactions,[55] linear-response approximation,[56] extended DH theory for asymmetric electrolytes,[57] mean-spherical approximation (MSA)[58] and symmetric PB and MSA.[59] Even though it has been argued by Overbeek and others[60] that the Sogami-Ise attraction[49] is due to inconsistencies in their thermodynamic treatment, the question does not seem to be settled yet and discussion is still in progress.[61] This attractive potential is in contrast to the generally accepted repulsive electrostatic component of the DLVO[34,35] pair potential between like-charged polyions. However, the purely repulsive nature of the polyion-polyion effective pair potential does not preclude *a priori* the existence of a liquid-gas separation, as has been shown by Roij *et al.*[53] The focus on the polyion-polyion effective interactions overlooks the important contribution to the free energy due to the polyion-microion interactions. Because most of the alternative analytical calculations to the Sogami-Ise attractive interaction potential requires some linearization procedure, the predicted liquid-gas coexistence should be analyzed with caution. In fact, these predictions disagree with simulation results in the presence of (explicit) *monovalent* counterions,[46,62] when no instabilities have been detected. Moreover, there are indications that the observed van der Waals-like loops are artifacts due to the linearization, these being drastically suppressed when nonlinearities are reintroduced in the theory by the use of renormalized charges.[63] Furthermore the linearization of the WS-cell semi-grand-canonical PB functional — which describes at the mean-field level the system in electrochemical equilibrium with an infinite salt reservoir — yields negative-compressibility, thermodynamically unstable regions which are absent in a full nonlinear treatment.[64,65] Although many aspects of these artifacts for the semi-grand-canonical case were already reported in the literature,[64] including a general analysis of the linearization scheme for various geometries,[65] we believe that there are still a few subtle points that need to be clarified.

The purpose of this paper is first to develop a linearization scheme suitable to the canonical (fixed amount of microions) case, by adopting an explicitly gauge-invariant approach. For the semi-grand-canonical case, it has been shown by Deserno and von Grünberg[65] that the occurrence of unstable linearized equations of state depends on the way the linearization scheme is performed and on the osmotic-pressure definition. By extending our gauge-invariant approach to the semi-grand-canonical ensemble, we try additionally to shed some light on this question. We argue that thermodynamic stability and consistency are in fact independent concepts. The gauge-invariant forms of the equations of state allow to establish an explicit correspondence between their nonlinear and linearized versions. The linearized equations, although thermodynamically self-consistent with quadratic expansions of the nonlinear ones, lead to artifacts when their underlying assumptions are not satisfied. We will show, by using gauge-invariant forms for the electrostatic potential, that there is a *unique* linearization (about the state-independent zero-th order Donnan densities) that corresponds to the minimization of the associated linearized semi-grand-canonical functional, which is also asymptotically exact (at the mean-field level) in the weak-coupling (high-temperature) limit. Therefore the expansion of the nonlinear functional about the state-independent Donnan densities, originally proposed for the spherical geometry by von Grünberg *et al.*[64] — and generalized for other geometries with analogous high symmetry in Ref. [65] — is not only "optimal", but it is asymptotically exact in the weak-coupling limit. In a companion paper[27] explicit analytical comparison is performed for the planar case, where the exact nonlinear solution (at the mean-field level) can be obtained.

The remainder of the paper is organized as follows. In Section 2 the salt-free model is introduced and the associated nonlinear equations are reviewed. In Section 3 the linearization of the appropriate functional is performed, considering three distinct physical situations: the salt-free (in the presence of neutralizing counterions only) system introduced in Section 2, with fixed amount of added monovalent salt (canonical ensemble) and in electrochemical equilibrium with an infinite monovalent salt reservoir (semi-grand-canonical ensem-

ble). In Section 4 we discuss our results in comparison to previous works[64,65] and present some concluding remarks in Section 5. Appendix A presents the boundary-density theorem (at the nonlinear mean-field level) for the salt-free simplest case. In Appendix B it is shown that the linearized Helmholtz free energy may be obtained by a Debye charging process of the linearized electrostatic energy. Appendix C presents the formal derivation of the linearized osmotic pressure for the salt-free case, showing that it corresponds to a quadratic expansion of the corresponding nonlinear osmotic pressure. In Appendices D and E it is shown that the linearized osmotic pressure in the presence of salt for the canonical and semi-grand-canonical ensembles, respectively, are given by the quadratic expansions of the corresponding nonlinear osmotic pressures. In Appendix F the self-consistent linearized averaged densities for the semi-grand-canonical ensemble are obtained by the minimization of the appropriate functional. In Appendix G we compare the linearized semi-grand-canonical osmotic pressures obtained by different schemes of the Legendre transformation connecting the canonical and semi-grand-canonical ensembles.

2 Definition of the model

Although the derivation of the PB equation from a free-energy density functional can be found elsewhere,[66,18,19] to introduce the notation and to stress the advantages of an explicitly gauge-invariant approach, it is essential to rederive it in the following. For simplicity, in this section only the salt-free case (in the presence of neutralizing counterions only) is presented. Generalization of the model including monovalent salt is straightforward and briefly described in Appendices D and E for the canonical and semi-grand-canonical cases, respectively.

The system to be considered is a hard charged sphere (spherical polyion) of radius a and total charge $-Zq$ distributed uniformly on its surface inside a concentric spherical WS cell of radius $R > a$, where $q > 0$ is the elementary charge and $Z \gg 1$ is the polyion valence. The radius R of the WS cell is related to the polyion density $n_{\rm p}$ such that the total volume of the suspension is equally distributed between the polyions, i.e. $n_{\rm p} \equiv \left(4\pi R^3/3\right)^{-1}$, whose hard cores occupy a fraction $\phi \equiv (a/R)^3$ of the total volume. To ensure the overall WS-cell charge neutrality, there are Z mobile (positive) point-like counterions, each carrying a charge $+q$, that are allowed to move in the spherical shell $a < |\boldsymbol{r}| \leq R$, whose volume reads

$$V = \int\limits_{a<|\boldsymbol{r}|\leq R} \mathrm{d}^3\boldsymbol{r} = \frac{4\pi}{3}\left(R^3 - a^3\right). \tag{1}$$

Henceforth, to simplify the notation, it will be implicit that all integrations are performed over the free volume V unoccupied by the polyion core — but also including the charged surface at $|\boldsymbol{r}| = a$ — unless otherwise stated. At the mean-field PB level the counterions are treated as an inhomogeneous ideal gas and are described by their (continuous) average local number density $n(\boldsymbol{r}) \equiv \left\langle\!\!\left\langle \sum_{i=1}^{Z} \delta^3\left(\boldsymbol{r} - \boldsymbol{r}_i\right) \right\rangle\!\!\right\rangle$, where δ^3 is the three-dimensional Dirac delta unction and the double brackets denote an ensemble (Boltzmann-weighted) average over all positions of the counterions. The total charge number density (counterions plus the negative surface charge on the sphere),

$$\rho(\boldsymbol{r}) = n(\boldsymbol{r}) - \frac{Z}{4\pi a^2}\delta^3(|\boldsymbol{r}| - a), \tag{2}$$

is related to the reduced electrostatic potential $\psi(\boldsymbol{r}) \equiv \beta q \Psi(\boldsymbol{r})$ by the (exact) Poisson equation,

$$\nabla^2\psi(\boldsymbol{r}) = -4\pi\ell_B\rho(\boldsymbol{r}), \tag{3}$$

where $\ell_B = \beta q^2/\epsilon$ is the Bjerrum length and $\beta^{-1} = k_B T$ is the thermal energy at temperature T. It is implicitly assumed that the solvent dielectric constant ϵ remains the same inside the sphere, so image-charge effects due to dielectric contrast are absent. The formal solution to the Poisson equation (3) may be written in terms of the Green function $G_3(\boldsymbol{r}, \boldsymbol{r}')$,

$$\psi(\boldsymbol{r}) = \ell_B \int \mathrm{d}^3\boldsymbol{r}'\, G_3(\boldsymbol{r}, \boldsymbol{r}')\, \rho(\boldsymbol{r}'), \qquad \nabla^2 G_3(\boldsymbol{r}, \boldsymbol{r}') = -4\pi\delta^3(\boldsymbol{r} - \boldsymbol{r}'), \tag{4}$$

which in turn allows us to express the mean-field Helmholtz free-energy functional $\mathscr{F}[n(\boldsymbol{r})]$ of a single WS cell as

$$\beta\mathscr{F}[n(\boldsymbol{r})] = \int \mathrm{d}^3\boldsymbol{r}\, n(\boldsymbol{r}) \left\{ \ln\left[n(\boldsymbol{r})\zeta^3\right] - 1 \right\} + \frac{\ell_B}{2} \int \mathrm{d}^3\boldsymbol{r}\, \mathrm{d}^3\boldsymbol{r}'\, \rho(\boldsymbol{r})\, G_3(\boldsymbol{r},\boldsymbol{r}')\, \rho(\boldsymbol{r}'), \tag{5}$$

where ζ is the thermal de Broglie wavelength of the counterions. It should be remarked that the mean-field Helmholtz free-energy functional (5) can be derived from the underlying PM Hamiltonian in different ways: as the saddle point of the action in a field-theoretic approach,[18] from a Gibbs-Bogoljubov inequality applied to a trial product state that decouples the original Hamiltonian[19] or from a first-cumulant expansion of the density functional reformulation of the associated partition function.[67] The first term of (5) represents the configurational entropy of the inhomogeneous ideal gas of counterions, while the second term corresponds to the electrostatic energy, which may be rewritten as

$$\begin{aligned} \beta U \,&=\, \frac{\ell_B}{2} \int \mathrm{d}^3\boldsymbol{r}\, \mathrm{d}^3\boldsymbol{r}'\, \rho(\boldsymbol{r})\, G_3(\boldsymbol{r},\boldsymbol{r}')\, \rho(\boldsymbol{r}') = \frac{1}{2} \int \mathrm{d}^3\boldsymbol{r}\, \psi(\boldsymbol{r})\rho(\boldsymbol{r}) \\ &=\, \frac{1}{8\pi\ell_B} \int \mathrm{d}^3\boldsymbol{r}\, \left[\nabla\psi(\boldsymbol{r})\right]^2 - \frac{1}{8\pi\ell_B} \oint_{\partial V} \psi(\boldsymbol{r})\, \nabla\psi(\boldsymbol{r}) \cdot \mathrm{d}\boldsymbol{S}. \end{aligned} \tag{6}$$

The surface contributions to the electrostatic energy — the last term of (6), performed over the boundary ∂V of the free volume V — vanish due to Gauss' law and the overall WS-cell charge neutrality,

$$\int \mathrm{d}^3\boldsymbol{r}\, \rho(\boldsymbol{r}) = 0, \qquad \text{or} \qquad \int \mathrm{d}^3\boldsymbol{r}\, n(\boldsymbol{r}) = Z. \tag{7}$$

The equilibrium counterion-density profile is obtained by minimizing the mean-field functional $\mathscr{F}[n(\boldsymbol{r})]$ with respect to $n(\boldsymbol{r})$ under the constraint of overall WS-cell charge neutrality (7). For this purpose it is convenient to introduce a translationally invariant (independent of $\boldsymbol{r}$) Lagrange multiplier $\beta\mu_{\mathrm{el}}$ and to define the extended Helmholtz free-energy functional including a Lagrange-multiplier term,

$$\tilde{\Omega}[n(\boldsymbol{r})] \equiv \mathscr{F} - \mu_{\mathrm{el}} \int \mathrm{d}^3\boldsymbol{r}\, \rho(\boldsymbol{r}) = \mathscr{F} - \mu_{\mathrm{el}} \left[\int \mathrm{d}^3\boldsymbol{r}\, n(\boldsymbol{r}) - Z \right], \tag{8}$$

which is the *analogue* of the conjugated semi-grand-canonical functional $\Omega[n(\boldsymbol{r})]$ in the case of non-fixed number of counterions (but fixed number of polyions). We should not confuse the *virtual* Lagrange multiplier μ_{el} with the *a priori* fixed chemical potential of counterions μ in the presence of an infinite counterion reservoir, when the natural choice for the thermodynamic ensemble is the semi-grand-canonical one,

$$\Omega \equiv \mathscr{F} - \mu \int \mathrm{d}^3\boldsymbol{r}\, n(\boldsymbol{r}), \qquad \int \mathrm{d}^3\boldsymbol{r}\, n(\boldsymbol{r}) \not\equiv Z. \tag{9}$$

The Helmholtz free-energy functional $\mathscr{F}$ supplemented by the Lagrange-multiplier term, $\tilde{\Omega} \neq \Omega$, *does not* correspond to the semi-grand-canonical functional Ω, because $\tilde{\Omega}$ and Ω are obtained under the constraints of a fixed number of counterions Z, and fixed chemical potential of counterions μ, respectively. Although this distinction may be seem rather academic, it is important to stress that overall charge neutrality (ensured by the Lagrange multiplier μ_{el}) and electrochemical equilibrium (imposed by a fixed chemical potential of counterions μ) are *independent* constraints. This prevents misinterpretations when treating the Donnan equilibrium (the system in electrochemical equilibrium with an infinite salt reservoir), when both constraints must be simultaneously satisfied.

Functional minimization of $\beta\tilde{\Omega}$ with respect to $n(\boldsymbol{r})$ leads to the Euler-Lagrange or stationary condition,[68]

$$\left.\frac{\delta\beta\tilde{\Omega}}{\delta n(\boldsymbol{r})}\right|_{n(\boldsymbol{r})=\bar{n}(\boldsymbol{r})} = \bar{\psi}(\boldsymbol{r}) + \ln\left[\bar{n}(\boldsymbol{r})\zeta^3\right] - \beta\bar{\mu}_{\mathrm{el}} = 0, \tag{10}$$

which yields the equilibrium counterion profile, $\bar{n}(\boldsymbol{r}) = \mathrm{e}^{\beta\bar{\mu}_{\mathrm{el}} - \bar{\psi}(\boldsymbol{r})}/\zeta^3$. In the above formulas the equilibrium electrostatic potential, $\bar{\psi}(\boldsymbol{r})$, is obtained by inserting the equilibrium counterion profile $\bar{n}(\boldsymbol{r})$ into $\psi(\boldsymbol{r})$, Eq. (4). The Boltzmann-weighted equilibrium counterion profile $\bar{n}(\boldsymbol{r})$, together with the Poisson equation (3), yields the nonlinear PB equation,

$$\nabla^2\bar{\psi}(\boldsymbol{r}) = -\frac{4\pi\ell_B}{\zeta^3}\mathrm{e}^{\beta\bar{\mu}_{\mathrm{el}} - \bar{\psi}(\boldsymbol{r})} + \frac{Z\ell_B}{a^2}\delta^3(|\boldsymbol{r}| - a), \tag{11}$$

where the equilibrium Lagrange multiplier,

$$\beta\bar{\mu}_{\rm el} = \ln\left(n_{\rm c}\zeta^3\right) - \ln\left\langle {\rm e}^{-\bar{\psi}(\boldsymbol{r})}\right\rangle, \tag{12}$$

is obtained by imposing the charge neutrality constraint (7). We introduced the *effective* average density of counterions in the free volume V unoccupied by the polyion core,

$$n_{\rm c} \equiv \langle \bar{n}(\boldsymbol{r})\rangle = \frac{Z}{V}, \tag{13}$$

the brackets denoting unweighted spatial averages over V,

$$\langle \mathcal{X}(\boldsymbol{r})\rangle \equiv \frac{\int {\rm d}^3\boldsymbol{r}\, \mathcal{X}(\boldsymbol{r})}{\int {\rm d}^3\boldsymbol{r}}, \tag{14}$$

in contrast to their *nominal* mean density in the suspension, $\tilde{n}_{\rm c} \equiv n_{\rm c}\,(1-\phi)$, which does not take into account the polyion hard cores. Note that the Lagrange multiplier (12) may be decomposed into two terms, a chemical potential corresponding to an ideal gas of uniform density $n_{\rm c}$ and an electrostatic contribution due to the counterion-cloud polarization, which may be written in terms of an average related to the equilibrium electrostatic potential $\bar{\psi}(\boldsymbol{r})$. We note that the presence of the Lagrange multiplier $\bar{\mu}_{\rm el}$ ensures *explicitly* the gauge invariance of the equations, that is, physical observables, like the equilibrium counterion-density profile,

$$\bar{n}(\boldsymbol{r}) = \frac{Z{\rm e}^{-\bar{\psi}(\boldsymbol{r})}}{\int {\rm d}^3\boldsymbol{r}\, {\rm e}^{-\bar{\psi}(\boldsymbol{r})}} = \frac{n_{\rm c}\exp\left[\langle\bar{\psi}\rangle - \bar{\psi}(\boldsymbol{r})\right]}{\left\langle\exp\left[\langle\bar{\psi}\rangle - \bar{\psi}(\boldsymbol{r})\right]\right\rangle}, \tag{15}$$

and the electric field, $\boldsymbol{E}(\boldsymbol{r}) = -\nabla\Psi(\boldsymbol{r}) = -(\beta q)^{-1}\nabla\bar{\psi}(\boldsymbol{r})$, *clearly* do not depend on a particular choice of the zero of the electrostatic potential $\bar{\psi}(\boldsymbol{r})$, since observables can always be written in terms of the gauge-invariant difference $\beta\bar{\mu}_{\rm el} - \bar{\psi}(\boldsymbol{r})$. In particular, explicitly gauge-invariant forms of the density profiles will be *useful* to establish a connection between the nonlinear and the linearized osmotic pressures (cf. Appendices C to E) and to derive the self-consistent linearized averaged densities for the semi-grand-canonical ensemble (cf. Appendix F). We should remark that — because consistent theories should always be gauge invariant — the use of *explicitly* gauge-invariant forms constitutes just a technical convenience, it does not represent an essential requirement. However, we believe that it provides a systematic and more transparent way to perform the calculations. Henceforth *gauge-invariant* will be a short-writing for *explicitly gauge-invariant,* unless otherwise stated.

The mean-field Helmholtz free energy (of a single WS cell) F is obtained by inserting the equilibrium density profile $\bar{n}(\boldsymbol{r})$, Eq. (15), into the mean-field functional $\mathscr{F}$, Eq. (5),

$$\begin{aligned}\beta F \,&\equiv\, \beta\mathscr{F}[\bar{n}(\boldsymbol{r})] = \frac{1}{2}\int {\rm d}^3\boldsymbol{r}\,\bar{\psi}(\boldsymbol{r})\bar{n}(\boldsymbol{r}) - \frac{1}{2}Z\bar{\psi}(a) + \int {\rm d}^3\boldsymbol{r}\,\bar{n}(\boldsymbol{r})\left\{\ln\left[\bar{n}(\boldsymbol{r})\zeta^3\right] - 1\right\}\\ &=\, Z\left[\beta\bar{\mu}_{\rm el} - 1 - \frac{1}{2}\bar{\psi}(a)\right] - \frac{1}{2}\int {\rm d}^3\boldsymbol{r}\,\bar{\psi}(\boldsymbol{r})\bar{n}(\boldsymbol{r}).\end{aligned} \tag{16}$$

In Appendix A it is shown that the (nonlinear) osmotic pressure P (over pure solvent), defined as the negative *total derivative* of the Helmholtz free energy F, Eq. (16), with respect to the WS-cell free volume[69] V, is simply given by

$$\beta P \,\equiv\, -\left.\frac{{\rm d}\beta F}{{\rm d}V}\right|_{Z,T} = \bar{n}(R), \tag{17}$$

which is the well-know WS-cell mean-field result that the salt-free osmotic pressure is related to the counterion boundary density.[23] This simple functional form still remains valid at the PM (beyond mean-field) level for WS-cells of various geometries,[70] although the mean-field prediction for the equilibrium boundary density $\bar{n}(R)$ will (in general) disagree with the corresponding rigorous PM result due to the neglect of intracell microion-microion correlations and finite ionic sizes. Henceforth, to simplify the notation, we will omit the bar to denote equilibrium properties.

3 Linearization scheme

3.1 In the presence of neutralizing counterions only

Let us define a linearized free-energy functional that will lead to DH-like equations of state for the salt-free model system introduced in the previous section. We start by expanding the PB Helmholtz free-energy functional (5) about the uniform counterion density (13), i.e., up to second order in the difference $n(\boldsymbol{r})-n_{\rm c}$,

$$\beta\mathscr{F}_{\rm DH} \,=\, Z\left[\ln\left(n_{\rm c}\zeta^3\right)-1\right]+\frac{1}{8\pi\ell_B}\int {\rm d}^3\boldsymbol{r}\,\left[\nabla\psi(\boldsymbol{r})\right]^2+\frac{1}{2}n_{\rm c}\int {\rm d}^3\boldsymbol{r}\,\left[\frac{n(\boldsymbol{r})}{n_{\rm c}}-1\right]^2. \tag{18}$$

The linear contribution is absent from (18), because it automatically vanishes,

$$\int {\rm d}^3\boldsymbol{r}\,\left[\frac{n(\boldsymbol{r})}{n_{\rm c}}-1\right]=\frac{Z}{n_{\rm c}}-V=0. \tag{19}$$

As in the previous section, we introduce a Lagrange multiplier $\mu_{\rm el}$ and define the extended Helmholtz free-energy functional $\tilde{\Omega}_{\rm DH}=\mathscr{F}_{\rm DH}-\mu_{\rm el}\int {\rm d}^3\boldsymbol{r}\,\rho(\boldsymbol{r})$. Functional minimization of $\tilde{\Omega}_{\rm DH}$ with respect to $n(\boldsymbol{r})$ leads to the linearized equilibrium counterion profile,

$$n(\boldsymbol{r})=n_{\rm c}\left[1+\beta\mu_{\rm el}-\psi(\boldsymbol{r})\right]. \tag{20}$$

It follows from Eqs. (19) and (20) that the linearized equilibrium Lagrange multiplier $\beta\mu_{\rm el}$ is given by the average electrostatic potential inside the WS cell,

$$\beta\mu_{\rm el}=\langle\psi(\boldsymbol{r})\rangle\,. \tag{21}$$

Inserting the equilibrium counterion-density profile (20) into the Poisson equation (3), leads to the DH-like equation,

$$\nabla^2\psi(\boldsymbol{r})=\kappa^2\left[\psi(\boldsymbol{r})-\beta\mu_{\rm el}-1\right]+\frac{Z\ell_B}{a^2}\delta^3(|\boldsymbol{r}|-a), \tag{22}$$

where the Debye screening length κ^{-1} is evaluated with the *uniform counterion density* $n_{\rm c}$,

$$\kappa=\kappa_{\rm c}\equiv\sqrt{4\pi\ell_B n_{\rm c}}. \tag{23}$$

This is different from the usual linearized-PB treatment of the spherical WS cell,[24] where the Debye screening length is defined in terms of the WS-cell boundary density $n(r=R)$. It should be remarked that the DH-like Eq. (22) leads to a *gauge-invariant* linearized solution, i.e., independent of the choice of the zero of the potential, because it depends only on the difference $\psi(\boldsymbol{r})-\beta\mu_{\rm el}$. This is not the case for the commonly used linearized-PB solution for the spherical WS cell,[71] when it is disputable how to construct a self-consistent associated linearized free energy, from which the linearized equations may be obtained by a functional minimization.

The solution of the linearized DH-like equation (22) for *an arbitrary* WS-cell boundary potential $\psi(R)$ and under the appropriate boundary conditions,

$$\left.\frac{{\rm d}\psi(r)}{{\rm d}r}\right|_{r=a}=\frac{Z\ell_B}{a^2},\qquad\text{and}\qquad\left.\frac{{\rm d}\psi(r)}{{\rm d}r}\right|_{r=R}=0, \tag{24}$$

reads

$$\psi(r) \,=\, \psi(R)+\frac{2Z\kappa\ell_B}{\Delta_2(\kappa R,\kappa a)}-\frac{Z\ell_B}{r}\,\frac{\Delta_1(\kappa R,\kappa r)}{\Delta_2(\kappa R,\kappa a)}, \tag{25}$$

$$\beta q\ell_B E(r) \,=\, -\ell_B\,\frac{{\rm d}\psi(r)}{{\rm d}r}=-\frac{Z\ell_B^2}{r^2}\frac{\Delta_2(\kappa R,\kappa r)}{\Delta_2(\kappa R,\kappa a)}, \tag{26}$$

$$\Delta_1(u,v) \,=\, \Delta_+(u){\rm e}^{v}-\Delta_-(u){\rm e}^{-v}, \tag{27}$$

$$\Delta_2(u,v) \,=\, \Delta_+(u)\Delta_-(v)-\Delta_-(u)\Delta_+(v), \tag{28}$$

$$\Delta_\pm(u) \,=\, (1\pm u){\rm e}^{\mp u}, \tag{29}$$

where the Lagrange multiplier $\beta\mu_{\rm el}$ is given by

$$\beta\mu_{\rm el} = \langle\psi(\boldsymbol{r})\rangle = \psi(R) + \frac{2Z\kappa\ell_B}{\Delta_2(\kappa R,\kappa a)} - 1. \tag{30}$$

Inserting the DH-like solution for the electrostatic potential (25) into the linearized Helmholtz free-energy functional (18) leads, after some algebra, to the linearized Helmholtz free energy,

$$\beta F_{\rm DH} \,=\, \beta\mathscr{F}_{\rm DH}[n(\boldsymbol{r})] = Z\left[\ln\left(n_{\rm c}\zeta^3\right) - \frac{3}{2}\right] + \frac{Z^2\ell_B}{2a}\,\frac{\Delta_1(\kappa R,\kappa a)}{\Delta_2(\kappa R,\kappa a)}. \tag{31}$$

In Appendix B it is shown that the linearized Helmholtz free energy (31) may also be obtained by a Debye charging process[10] of the linearized electrostatic energy, confirming thus its thermodynamic self-consistency.

The linearized osmotic pressure (over pure solvent) of the colloidal suspension follows from the negative *total derivative* of the linearized Helmholtz free energy (without including the Lagrange multiplier term) with respect to the WS-cell free volume V,

$$\begin{aligned}\beta P_{\rm DH} = -\left.\frac{{\rm d}\beta F_{\rm DH}}{{\rm d}V}\right|_{Z,T} &= n_{\rm c} - \frac{Z^2\ell_B}{2a}\,\frac{\rm d}{{\rm d}V}\left[\frac{\Delta_1(\kappa R,\kappa a)}{\Delta_2(\kappa R,\kappa a)}\right]_{Z,T} = n_{\rm c}\left\{1 + \frac{Z\kappa\ell_B}{4\Delta_2^2(\kappa R,\kappa a)}\times\right.\\ &\left.\times\,\left[\frac{\Delta_1(\kappa R,\kappa a)}{\kappa a}\left[\Delta_1(\kappa R,\kappa a) - \Delta_2(\kappa R,\kappa a)\right] - 4\kappa a\left(1 + \frac{2}{3}\kappa^2a^2 - \kappa^2R^2\right) - \frac{4}{3}\kappa^3R^3\right]\right\},\end{aligned} \tag{32}$$

where one should take into account both the explicit R dependence as well as the volume dependence of the screening length κ^{-1} when computing the total derivative. The first term of (32) represents the uniform counterion-density ideal-gas law, while the next term corresponds to the mean-field electrostatic corrections[72] due to *intracell* polyion-microion correlations. In Appendix C it is shown that the linearized osmotic pressure (32) can be also obtained by a *formal* differentiation of the linearized Helmholtz free energy and that it also corresponds to a quadratic expansion of the nonlinear PB osmotic pressure (17). At the end of the next subsection — that considers the system in the presence of added salt — we shall find that for sufficiently large surface charges the linearized osmotic pressure (32) is no longer a monotonic function of the WS-cell free volume V, which would imply a thermodynamical instability and an associated phase separation of the system — in contrast to the full nonlinear theory, which does not predict any instability.

3.2 In the presence of neutralizing counterions and added salt (canonical ensemble)

Let us now add a symmetric monovalent (1:1) salt to the system. At the same level of mean-field approximation, all microions are treated as inhomogeneous ideal gases, described by their average local number densities $n_\pm(\boldsymbol{r})$. We will not distinguish between counterions and positive ions derived from the salt dissociation. Therefore $n_+(\boldsymbol{r})$ accounts both for counterions and positive salt ions (cations), while $n_-(\boldsymbol{r})$ represents the negative coions (anions). In terms of these number densities, the total charge number density reads

$$\rho(\boldsymbol{r}) = n_+(\boldsymbol{r}) - n_-(\boldsymbol{r}) - \frac{Z}{4\pi a^2}\delta^3\left(|\boldsymbol{r}| - a\right). \tag{33}$$

The effective average uniform densities of positive and negative microions are given by

$$\bar{n}_\pm = \langle n_\pm(\boldsymbol{r})\rangle = \frac{Q_\pm}{V}, \qquad\qquad Q_+ = Z + n_{\rm s}V, \qquad\qquad Q_- = n_{\rm s}V, \tag{34}$$

where $n_{\rm s}$ is the *a priori* known effective average salt concentration and $Q_\pm$ are the fixed total number of positive and negative microions inside a WS cell. Within the cell-model approximation the salt ions are evenly distributed between different cells and the average salt concentration $n_{\rm s}$ is the same for each identical WS cell. For later convenience, it will be useful to introduce the dimensionless parameter

$$s \equiv \frac{Q_-}{Z} = \frac{n_{\rm s}}{n_{\rm c}}, \tag{35}$$

which measures the contribution of the salt ions to the ionic strength in the suspension,

$$I \equiv \frac{1}{2}\left(n_{\rm c}+2n_{\rm s}\right)=\frac{1}{2}\left(1+2s\right)n_{\rm c}. \tag{36}$$

For example, for $s=1$ there is one pair of salt ions for each positive counterion in solution.

We expand the nonlinear PB Helmholtz free-energy functional,

$$\beta\mathscr{F}[n_{\pm}(\boldsymbol{r})]\,=\,\frac{1}{8\pi\ell_B}\int{\rm d}^3\boldsymbol{r}\,\left[\nabla\psi(\boldsymbol{r})\right]^2+\sum_{i=\pm}\int{\rm d}^3\boldsymbol{r}\,n_i(\boldsymbol{r})\left\{\ln\left[n_i(\boldsymbol{r})\zeta_i^3\right]-1\right\}, \tag{37}$$

about the average uniform densities (34), up to second order in the differences $n_{\pm}(\boldsymbol{r})-\bar{n}_{\pm}$,

$$\beta\mathscr{F}_{\rm DH}\,=\,\sum_{i=\pm}Q_i\left[\ln\left(\bar{n}_i\zeta_i^3\right)-1\right]+\frac{1}{8\pi\ell_B}\int{\rm d}^3\boldsymbol{r}\,\left[\nabla\psi(\boldsymbol{r})\right]^2+\frac{1}{2}\sum_{i=\pm}\bar{n}_i\int{\rm d}^3\boldsymbol{r}\left[\frac{n_i(\boldsymbol{r})}{\bar{n}_i}-1\right]^2, \tag{38}$$

where $\zeta_{\pm}$ are the thermal de Broglie wavelengths of cations (including the positive counterions) and anions, respectively. We introduce a Lagrange multiplier $\mu_{\rm el}$, which will ensure the overall WS-cell charge neutrality,

$$\int{\rm d}^3\boldsymbol{r}\,\rho(\boldsymbol{r})=0, \qquad\qquad \text{or} \qquad\qquad \int{\rm d}^3\boldsymbol{r}\,\left[n_+(\boldsymbol{r})-n_-(\boldsymbol{r})\right]=Z, \tag{39}$$

and define the extended Helmholtz free-energy functional, $\tilde{\Omega}_{\rm DH}=\mathscr{F}_{\rm DH}-\mu_{\rm el}\int{\rm d}^3\boldsymbol{r}\,\rho(\boldsymbol{r})$. Functional minimization of $\tilde{\Omega}_{\rm DH}$ with respect to $n_{\pm}(\boldsymbol{r})$ leads to the equilibrium density profiles,

$$n_{\pm}(\boldsymbol{r})=\bar{n}_{\pm}\left[1\pm\beta\mu_{\rm el}\mp\psi(\boldsymbol{r})\right]. \tag{40}$$

Using (34) and (40), we obtain that the Lagrange multiplier is given by the average electrostatic potential inside the WS cell, $\beta\mu_{\rm el}=\langle\psi(\boldsymbol{r})\rangle$, as in the salt-free case, Eq. (21). Inserting the equilibrium profiles (40) into the Poisson equation (3), leads to the DH-like equation,

$$\nabla^2\psi(\boldsymbol{r})\,=\,\kappa^2\left[\psi(\boldsymbol{r})-\beta\mu_{\rm el}-\frac{1}{1+2s}\right]+\frac{Z\ell_B}{a^2}\delta^3(|\boldsymbol{r}|-a), \tag{41}$$

where the inverse of the Debye screening length is now given by

$$\kappa=\sqrt{8\pi\ell_B I}=\sqrt{4\pi\ell_B(1+2s)n_{\rm c}}=\kappa_{\rm c}\sqrt{1+2s}. \tag{42}$$

Solving the associated linearized DH-like equation leads again to the electrostatic potential (25), with the Lagrange multiplier for an arbitrary cell-boundary electrostatic potential $\psi(R)$ given by

$$\beta\mu_{\rm el}=\langle\psi(\boldsymbol{r})\rangle=\psi(R)+\frac{2Z\kappa\ell_B}{\Delta_2(\kappa R,\kappa a)}-\frac{1}{1+2s}. \tag{43}$$

At this point we should remark that — in the infinite-dilution limit ($R\to\infty, n_{\rm c}\to 0$), but in the presence of excess salt ($s\to\infty$, finite $n_{\rm s}$) — the linearized electrostatic potential $\psi(r)$ reduces to the Yukawa screened electrostatic potential,

$$\lim_{\substack{R\to\infty\\ s\to\infty}}\left[\psi(r)-\psi(R)\right]=-\frac{Z\ell_B{\rm e}^{-\kappa(r-a)}}{(1+\kappa a)\,r}, \qquad \kappa=\sqrt{8\pi\ell_B n_{\rm s}}, \tag{44}$$

which leads to the repulsive electrostatic component of the traditional DLVO interaction potential[34,35] between two identical spherical particles of radius a whose centers are a distance r apart,

$$W(r)=Z^2\ell_B\left(\frac{{\rm e}^{\kappa a}}{1+\kappa a}\right)^2\frac{{\rm e}^{-\kappa r}}{r}. \tag{45}$$

The phase diagram and dynamical properties of a suspension of spherical particles interacting through the effective DLVO pairwise potential (45) were systematically investigated in Ref. [73] using molecular

and lattice dynamics techniques. We should note that the polyion-polyion interaction potential within the traditional (symmetric) DH framework may be obtained from the *exact* (non-spherically symmetric) solution of the Helmholtz equation $\nabla^2\psi(\boldsymbol{r}) = \kappa^2\psi(\boldsymbol{r})$ for two spherical charged particles.[74] The large-separation ($r \to \infty$) asymptotics of this pairwise potential leads directly to the DLVO interaction potential (45). One should also keep in mind that the exact limiting laws (within the RPM) of the underlying DH theory[10] — associated with the Helmholtz equation — are only valid in the asymptotic limit of vanishing ionic strengths ($\kappa \to 0$). Most likely this exactness does not apply for the asymmetric case of strongly charged colloids. Alternatively, the DLVO interaction potential (45) may also be obtained by the large-separation asymptotics of the microion-averaged polyion-polyion potential of mean-force, obtained using the MSA integral equation for the polyion- and the microion-microion correlations in the PM.[75]

Inserting the equilibrium density profiles (40) into the linearized Helmholtz free-energy functional $\mathscr{F}_{\rm DH}[n_\pm(\boldsymbol{r})]$, Eq. (38), leads to the linearized Helmholtz free energy,

$$\begin{aligned}\beta F_{\rm DH} = \beta\mathscr{F}_{\rm DH}[n_\pm(\boldsymbol{r})] \,=\, & (1+s)Z\left\{\ln\left[(1+s)n_{\rm c}\zeta_+^3\right]-1\right\} + sZ\left[\ln\left(sn_{\rm c}\zeta_-^3\right)-1\right] \\ & + \frac{Z}{2}\left[\frac{Z\ell_B}{a}\,\frac{\Delta_1(\kappa R,\kappa a)}{\Delta_2(\kappa R,\kappa a)} - \frac{1}{1+2s}\right].\end{aligned} \tag{46}$$

The two first terms of (46) correspond to the ideal-gas entropy of the uniform expansion densities $\bar{n}_\pm$, while the last term represents the linearized excess Helmholtz free energy due to the polarization of the microionic cloud around the polyion. In the infinite-dilution limit and in the presence of excess salt ($R \to \infty, n_{\rm c} \to 0$, but finite $n_{\rm s}$),

$$\lim_{\substack{R\to\infty\\ s\to\infty}} \frac{Z}{2}\left[\frac{Z\ell_B}{a}\,\frac{\Delta_1(\kappa R,\kappa a)}{\Delta_2(\kappa R,\kappa a)} - \frac{1}{1+2s}\right] = \frac{Z^2\ell_B}{2a\,(1+\kappa a)}, \qquad \kappa = \sqrt{8\pi\ell_B n_{\rm s}}, \tag{47}$$

it coincides with the polyion-counterion interaction free energy (including the polyion self-energy) obtained in an extended Debye-Hückel-Bjerrum approach for colloidal suspensions — cf. Eq. (2) of Ref. [12]. The asymptotic *electrostatic excess free energy* (47), obtained by linearization of the PB WS-cell model functional, accidentally[76] coincides with the *electrostatic work* done in charging up the surface of the polyion against the ionic atmosphere in the framework of the traditional DH theory — cf. Ref. [9], pp.339 — which is obtained by a Güntelberg charging process. The Güntelberg[77] and the Debye[10] charging processes differ by the fact that in the latter the *whole system* (including the ionic atmosphere) is simultaneously charged.

The connection between the infinite-dilution ($R \to \infty$) limit of the linearized excess Helmholtz free energy (46),

$$\lim_{\substack{R\to\infty\\ \text{finite } s}} \frac{Z}{2}\left[\frac{Z\ell_B}{a}\,\frac{\Delta_1(\kappa R,\kappa a)}{\Delta_2(\kappa R,\kappa a)} - \frac{1}{1+2s}\right] = \frac{Z}{2}\left[\frac{Z\ell_B}{a(1+\kappa a)} - \frac{1}{1+2s}\right], \tag{48}$$

and the state-independent volume terms obtained by Roij *et al.*[53] was first reported by Warren, cf. Eqs. (7) and (11) of Ref. [55], followed by Denton, cf. Eq. (55) of Ref. [56]. Subtracting out from Eq. (48) the polyion self-energy, $Z^2\ell_B/(2a)$, yields the negative contributions of the state-independent volume terms obtained by Roij *et al.* — cf. Eq. (61) of Ref. [53],

$$\frac{Zn_{\rm p}}{2}\left[\frac{Z\ell_B}{a(1+\kappa a)} - \frac{1}{1+2s}\right] - \frac{Z^2\ell_B}{2a}n_{\rm p} = -\frac{Z^2\ell_B}{2}\,\frac{n_{\rm p}\kappa}{1+\kappa a} - \frac{2\pi\ell_B}{\kappa^2}\left(Zn_{\rm p}\right)^2, \tag{49}$$

recalling that $n_{\rm p} = \left(4\pi R^3/3\right)^{-1}$ is the polyion density of the suspension. It has been claimed[53] that these volume-dependent (but state-independent) negative contributions to the Helmholtz free energy are responsible for driving a gas-liquid phase separation in dilute deionized aqueous colloidal suspensions.

The linearized *canonical* osmotic pressure of the colloidal suspension follows from the negative *total derivative* of the linearized Helmholtz free energy (without including the Lagrange multiplier term) with respect to the WS-cell free volume V, but keeping fixed the total amount of salt,

$$\begin{aligned}\beta P_{\rm DH}^{\rm can}(\phi,s) \,=\, & -\left.\frac{{\rm d}\beta F_{\rm DH}}{{\rm d}V}\right|_{Z,T,s} = (1+2s)n_{\rm c} - \frac{Z^2\ell_B}{2a}\,\frac{\rm d}{{\rm d}V}\left[\frac{\Delta_1(\kappa R,\kappa a)}{\Delta_2(\kappa R,\kappa a)}\right]_{Z,T,s} \\ \,=\, & (1+2s)n_{\rm c}\left\{1 + \frac{Z\kappa\ell_B}{4(1+2s)\Delta_2^2(\kappa R,\kappa a)}\left[\frac{\Delta_1(\kappa R,\kappa a)}{\kappa a}\times\right.\right.\end{aligned}$$

$$\times\ [\Delta_1(\kappa R,\kappa a)-\Delta_2(\kappa R,\kappa a)]-4\kappa a\left(1+\frac{2}{3}\kappa^2a^2-\kappa^2R^2\right)-\frac{4}{3}\kappa^3R^3\Bigg]\Bigg\}. \tag{50}$$

In Appendix D it is shown that the linearized canonical osmotic pressure (50) corresponds to a quadratic expansion of the nonlinear PB canonical osmotic pressure (D5).

In the vanishing volume fraction of polyions (infinite-dilution) limit, $\phi=(a/R)^3\to 0$, the linearized canonical osmotic pressure has the asymptotic behaviour

$$\beta P_{\rm DH}^{\rm can}=\frac{\theta\,(1+2s)\,\phi}{4\pi a^2\ell_B}\left[1-\frac{\theta}{10\,(1+2s)}\phi^{1/3}-\frac{4\theta^2}{175}\phi^{2/3}+\mathscr{O}\left(\phi\right)\right],\qquad \theta\equiv\frac{3Z\ell_B}{a}, \tag{51}$$

which leads to the asymptotic linearized inverse isothermal compressibility,

$$\beta\chi_{\rm DH}^{-1}\equiv n_{\rm p}\frac{{\rm d}\beta P_{\rm DH}^{\rm can}}{{\rm d}n_{\rm p}}=Zn_{\rm p}\,(1+2s)\left[1-\frac{2\theta}{15\,(1+2s)}\phi^{1/3}-\frac{4\theta^2}{105}\phi^{2/3}+\mathscr{O}\left(\phi\right)\right]. \tag{52}$$

In contrast to the semi-grand-canonical case (to be treated in the next subsection), the linearized isothermal compressibility in the canonical ensemble is stable in the infinite-dilution limit, $\lim_{\phi\to 0}\chi_{\rm DH}>0$. However, as shown in Figures 1 and 2, for finite densities ($\phi\neq 0$) and sufficiently large values of θ, the linearized canonical osmotic pressure $\beta P_{\rm DH}^{\rm can}$ is no longer a convex function of the volume fraction ϕ, implying thus the onset of a thermodynamical instability. For salt-free suspensions ($s=0$), the associated critical point — represented by the black circle in Figure 2 — is located at

$$\phi_{\rm crit}=0.008586189\cdots,\qquad \theta_{\rm crit}=44.902477094\cdots, \tag{53}$$

which is determined by the criticality condition ${\rm d}P_{\rm DH}^{\rm can}/{\rm d}\phi={\rm d}^2P_{\rm DH}^{\rm can}/{\rm d}\phi^2=0$. We should stress that the coexistence regions between the dilute gas (G) and the dense liquid (L) phases — not shown in Figure 2 — must be determined under the constraints of constant chemical potential of polyions $\mu_{\rm p}$ and of salt particles $\mu_{\rm s}$. For example, the salt-free bimodal line that defines the boundary of the coexistence region is given by the coupled system of equations,

$$P_{\rm DH}^{\rm can}(\phi_{\rm G},s=0)\,=\,P_{\rm DH}^{\rm can}(\phi_{\rm L},s=0),\qquad\qquad \mu_{\rm p}(\phi_{\rm G},s=0)=\mu_{\rm p}(\phi_{\rm L},s=0), \tag{54}$$

where $\mu_{\rm p}(\phi,s=0)$ is the salt-free chemical potential of the polyions,

$$\mu_{\rm p}(\phi,s=0)\equiv\frac{\rm d}{{\rm d}n_{\rm p}}\left[\frac{F_{\rm DH}}{\tilde{V}}\right]_{s=0}=F_{\rm DH}(\phi,s=0)+\frac{P_{\rm DH}^{\rm can}(\phi,s=0)}{n_{\rm p}(\phi)}, \tag{55}$$

and $\tilde{V}\equiv 4\pi a^3/(3\phi)=1/n_{\rm p}$ is the total WS-cell volume. Because the critical behaviour is a spurious result of the linearization, it is not worthwhile to construct the phase diagrams in detail and we restrict ourselves only to present the spinodal lines in Figure 2. This, however, will not change the location of the critical points, where the bimodal and the spinodal lines meet. Addition of salt *stabilizes* the suspension by reducing the unstable region to higher values of θ, as also illustrated by the $s\neq 0$ spinodal lines in Figure 2. The corresponding bimodal lines are determined by generalizing Eqs. (54) to the case of added salt ($s\neq 0$),

$$P_{\rm DH}^{\rm can}(\phi_{\rm G},s)\,=\,P_{\rm DH}^{\rm can}(\phi_{\rm L},s),\qquad\qquad \mu_{\rm p}(\phi_{\rm G},s)=\mu_{\rm p}(\phi_{\rm L},s), \tag{56}$$

where the chemical potential of the polyions in presence of added salt, $\mu_{\rm p}(\phi,s\neq 0)$, is given by Eq. (G6). With added salt, there is (in the coexistence region) a redistribution of microion pairs between the dilute and the dense phases, which still obeys the WS-cell charge-neutrality constraint (39). Hence, inside the coexistence region ($\phi_{\rm G}\leq\phi\leq\phi_{\rm L}$) the two fluid phases will not have the same value of s (corresponding to the homogeneous system). Their values in the gas ($s_{\rm G}$) and the liquid ($s_{\rm L}$) phases are obtained by imposing the total conservation of salt particles,

$$s=\frac{\phi_{\rm L}\,(\phi-\phi_{\rm G})}{\phi\,(\phi_{\rm L}-\phi_{\rm G})}s_{\rm L}+\frac{\phi_{\rm G}\,(\phi_{\rm L}-\phi)}{\phi\,(\phi_{\rm L}-\phi_{\rm G})}s_{\rm G},\qquad\qquad \phi_{\rm G}\leq\phi\leq\phi_{\rm L}, \tag{57}$$

and the equality in both fluid phases of the chemical potential of salt particles $\mu_{\rm s}(\phi,s)$ — as given by Eq. (G5),

$$\mu_{\rm s}(\phi_{\rm G},s_{\rm G})=\mu_{\rm s}(\phi_{\rm L},s_{\rm L}). \tag{58}$$

An important and useful concept in charged colloidal systems is the charge renormalization[78,79] of the polyion bare charge Z for finite volume fractions ϕ. For highly charged polyions, i.e. in the $\sigma \equiv Z/(4\pi a^2) \to \infty$ limit, it has been shown by Alexander *et al.*[24] that the renormalized effective charge $Z_{\rm eff}$ in the salt-free system approaches a saturation value $Z_{\rm sat} \approx aw(\phi)/\ell_B$, with $w(\phi)$ assuming numerical values[24,80] around 9 to 15 in the volume-fraction range $0.01 \leq \phi \leq 0.1$. A self-consistent linearized osmotic pressure including charge renormalization effects would require the inclusion of additional terms due to the volume-fraction dependence of the effective charge $Z_{\rm eff} = Z_{\rm eff}(V)$, since the osmotic pressure is defined as the negative *total derivative* of the Helmholtz free energy with respect to the volume V. In other words, the linearized canonical osmotic pressure $P_{\rm DH}^{\rm can}$ taking into account charge-renormalization effects *is not simply* given by replacing $Z \to Z_{\rm eff}$ into Eq. (50). This point will be considered in a future work.[81] It is interesting to note, however, that the linearized critical threshold $\theta_{\rm crit}$ given by Eq. (53) is very close to the (largest) salt-free saturation ($Z \to \infty$) effective charge $\theta_{\rm sat} = 3Z_{\rm sat}\ell_B/a \approx 45$ determined by Alexander *et al.*[24] It has been speculated[15] that this curious coincidence drives suspensions of highly charged colloids close to criticality. This might account for some of the experimental findings in dilute deionized aqueous suspensions of highly charged colloids,[41,42,43] which then would be explained by the presence of strong density fluctuations near the criticality.[15] Another consequence that effective charges are below the saturation value, and therefore also below the linearized critical threshold, is that charge renormalization would stabilize the suspension against phase separation, because the unstable region predicted by linearized theory is unreachable (or at least drastically reduced) when including renormalized effective charges. This fact was pointed out previously[63] using a generalized Debye-Hückel-Bjerrum approach for charged colloidal suspensions. In the present calculation, however, the critical behaviour is an artifact of the linearization, which is absent in the full nonlinear treatment. Therefore, the occurrence of a thermodynamical instability can only be explained beyond the WS-cell mean-field approximation, by including excluded-volume effects, *intercell* polyion-microion and microion-microion correlations that are neglected in the WS-cell mean-field PB picture.

3.3 In contact with an infinite salt reservoir (semi-grand-canonical ensemble)

Let us now consider the colloidal suspension in electrochemical equilibrium with an infinite salt reservoir of fixed bulk density $n_{\rm b}$. The suspension is separated from the infinite reservoir by a semi-permeable membrane. The solvent and microions (counterions and salt ions) can pass through the membrane, but not the large polyions. This gives rise to an imbalance in the osmotic pressure across the semi-permeable membrane. This equilibrium between the suspension and the salt reservoir is referred to as a Donnan equilibrium.[83,84,9,85] Like in the previous subsections we will consider only the case of monovalent counterions and symmetric monovalent (1:1) salt.

The effective average salt concentration in the colloidal suspension, $n_{\rm s} \equiv \langle n_-(\boldsymbol{r})\rangle$, does not coincide with the reservoir bulk density $n_{\rm b}$ and is not known *a priori*. A nontrivial question is its dependence with the physical parameters of the system, e.g., bulk salt concentration $n_{\rm b}$, polyion radius a, polyion valence Z and volume fraction $\phi \equiv (a/R)^3$. At the WS-cell PB mean-field level of approximation this problem has already been considered in the literature[86,87] and it is summarized in Appendix E. Compared to the canonical case treated in the previous subsection — when the amount of microions is fixed and known *a priori* — there are two main differences. First, because the Donnan equilibrium is established under constant electrochemical potential of microions, the natural thermodynamical ensemble to perform the calculations is the semi-grand-canonical one,

$$\Omega_{\rm DH} \equiv \mathscr{F}_{\rm DH} - \sum_{i=\pm}\mu_i\int {\rm d}^3\boldsymbol{r}\, n_i(\boldsymbol{r}), \qquad\qquad \beta\mu_\pm = \ln\left(n_{\rm b}\zeta_\pm^3\right), \tag{59}$$

where we impose the equality of the microion electrochemical potentials inside the colloidal suspension, $\mu_\pm$, to the (mean-field) chemical potential of ideal gases of uniform density $n_{\rm b}$ for both types of ions in the infinite salt reservoir, $\beta^{-1}\ln\left(n_{\rm b}\zeta_\pm^3\right)$. The second difference is that the effective average uniform densities of positive and negative ions, about which the linearization should be performed, vary in a nontrivial way as the WS-cell free volume V is changed. In Appendix F it is shown that the self-consistent linearized average densities for the Donnan problem are given by the state-independent zero-th order Donnan densities,

$$\bar{n}_\pm = \frac{\sqrt{n_{\rm c}^2 + (2n_{\rm b})^2} \pm n_{\rm c}}{2}, \tag{60}$$

where $n_{\rm c}$ is the effective averaged counterion density, defined in (13). These correspond to the uniform densities that the system would have in the infinite-temperature ($\ell_B = 0$) limit under the constraint of overall WS-cell charge neutrality (39). We should remark that they *do not* correspond to the effective averages of the full nonlinear PB densities (E3),

$$\langle n_{\pm}(\boldsymbol{r})\rangle = \frac{\sqrt{n_{\rm c}^2 + (2n_{\rm b})^2 \left\langle {\rm e}^{\psi(\boldsymbol{r})}\right\rangle \left\langle {\rm e}^{-\psi(\boldsymbol{r})}\right\rangle} \pm n_{\rm c}}{2} = \frac{\sqrt{n_{\rm c}^2 + (2n_{\rm b})^2 {\rm e}^{\langle \delta_2(\boldsymbol{r})\rangle} + \mathscr{O}\left[\langle \delta_3(\boldsymbol{r})\rangle\right]} \pm n_{\rm c}}{2}, \tag{61}$$

because of the nonvanishing quadratic and higher-order ($\nu \geq 2$) contributions of the electrostatic potential differences,

$$\delta_{\nu}(\boldsymbol{r}) \equiv \left[\langle\psi\rangle - \psi(\boldsymbol{r})\right]^{\nu}. \tag{62}$$

Here one can see an advantage of the gauge-invariant formulation of the problem: the linearized expansion densities (60) are simply obtained by taking the potential-independent, infinite-temperature ($\ell_B = 0$) limit of the PB nonlinear averaged densities (61), when the electrostatic potential differences vanish, $\lim_{\ell_B \to 0} \delta_{\nu}(\boldsymbol{r}) \to 0$. It is also clear that any other choice for the expansion densities will not lead to the exact potential-independent (infinite-temperature) limit of the nonlinear equations. As also derived in Appendix F, the Donnan average densities, Eqs. (60), do indeed correspond to the functional minimization of the corresponding linearized semi-grand-canonical functional. We note that Deserno and von Grünberg[65] define an optimal linearization point $\bar{\psi}_{\rm opt}$ — related to the above gauge-invariant expansion densities by $\bar{n}_{\pm} = n_{\rm b}{\rm e}^{\mp\bar{\psi}_{\rm opt}}$ — by using arguments based on the plausibility of this choice. They show that any other choice for the linearization point would lead to conflicting inequalities involving nonlinear and linearized averages. Finally, we should mention that even though the uniform expansion densities (60) are *internally* self-consistent (within the semi-grand-canonical ensemble) with the linearized truncation of the quadratic expansion of the nonlinear semi-grand-canonical functional, *global* self-consistency (between the canonical and the semi-grand-canonical ensembles) will require the use of the quadratic truncation of the nonlinear averages (61) as the self-consistent averaged densities, as discussed in detail in Appendix G. The inclusion of the quadratic contributions into the expansion averages, however, do not improve the agreement between the linearized and nonlinear equations, as can be shown by the explicit analytical comparison in the exactly solvable planar case.[27]

Once again, we introduce a Lagrange multiplier $\mu_{\rm el}$ that enforces the overall WS-cell charge-neutrality (39), and define the extended semi-grand-canonical functional, $\tilde{\Omega}_{\rm DH} = \Omega_{\rm DH} - \mu_{\rm el}\int {\rm d}^3\boldsymbol{r}\,\rho(\boldsymbol{r})$. Functional minimization of $\tilde{\Omega}_{\rm DH}$ with respect to $n_{\pm}(\boldsymbol{r})$, performed in Appendix F, leads to the self-consistent linearized averaged densities (60) and the linearized equilibrium profiles,

$$n_{\pm}(\boldsymbol{r}) = \bar{n}_{\pm}\left[1 \pm \langle\psi(\boldsymbol{r})\rangle \mp \psi(\boldsymbol{r})\right]. \tag{63}$$

We should remark that, contrary to the salt-free and canonical cases, cf. Eq. (21), here the equilibrium Lagrange multiplier $\beta\mu_{\rm el}$ *is not* related to the average electrostatic potential, $\beta\mu_{\rm el} \neq \langle\psi(\boldsymbol{r})\rangle$.

Inserting the linearized equilibrium profiles (63) into the Poisson equation (3), leads to the DH-like equation,

$$\nabla^2\psi(\boldsymbol{r}) = \kappa^2\left[\psi(\boldsymbol{r}) - \langle\psi(\boldsymbol{r})\rangle - \eta\right] + \frac{Z\ell_B}{a^2}\delta^3(|\boldsymbol{r}| - a), \tag{64}$$

where the parameter

$$\eta \equiv \frac{\bar{n}_+ - \bar{n}_-}{\bar{n}_+ + \bar{n}_-} = \frac{n_{\rm c}}{\sqrt{n_{\rm c}^2 + (2n_{\rm b})^2}}, \tag{65}$$

measures the relative importance of the counterions to the ionic strength in the colloidal suspension,

$$I \equiv \frac{1}{2}\left(\bar{n}_+ + \bar{n}_-\right) = \frac{1}{2}\sqrt{n_{\rm c}^2 + (2n_{\rm b})^2} = \frac{n_{\rm c}}{2\eta} = \frac{n_{\rm b}}{\sqrt{1-\eta^2}}. \tag{66}$$

Furthermore, the (effective) Debye screening length κ^{-1} in the colloidal suspension,

$$\kappa^2 = 8\pi\ell_B I = \frac{\kappa_{\rm c}^2}{\eta} = \frac{\kappa_{\rm b}^2}{\sqrt{1-\eta^2}} > \kappa_{\rm b}^2, \tag{67}$$

is always shorter than the Debye screening length $\kappa_{\rm b}^{-1} \equiv 1/\sqrt{8\pi\ell_B n_{\rm b}}$ associated with the bulk salt concentration $n_{\rm b}$ in the reservoir, showing that screening is enhanced in the colloidal suspension compared to the salt reservoir.

Solving the associated linearized DH-like equation (64) leads again to the electrostatic potential (25), with the average electrostatic potential over the WS-cell volume for an arbitrary cell-boundary electrostatic potential $\psi(R)$ given by

$$\langle\psi(\boldsymbol{r})\rangle = \psi(R) + \frac{2Z\kappa\ell_B}{\Delta_2(\kappa R,\kappa a)} - \eta. \tag{68}$$

In close analogy to the linearized Helmholtz free energy for the canonical case, Eq. (46), the final expression for the linearized semi-grand-canonical potential is

$$\begin{aligned}\beta\Omega_{\rm DH} = \beta\Omega_{\rm DH}[n_\pm(\boldsymbol{r})] &= \sum_{i=\pm} V\bar{n}_i\left[\ln\left(\frac{\bar{n}_i}{n_{\rm b}}\right)-1\right] + \frac{Z}{2}\left[\frac{Z\ell_B}{a}\,\frac{\Delta_1(\kappa R,\kappa a)}{\Delta_2(\kappa R,\kappa a)} - \eta\right]\\ &= Z\left[\operatorname{arctanh}\eta - \frac{1}{\eta} - \frac{\eta}{2} + \frac{Z\ell_B}{2a}\,\frac{\Delta_1(\kappa R,\kappa a)}{\Delta_2(\kappa R,\kappa a)}\right].\end{aligned} \tag{69}$$

The linearized *semi-grand-canonical* osmotic pressure follows from the negative *total derivative* of the linearized semi-grand-canonical potential (without including the Lagrange multiplier term associated with $\mu_{\rm el}$) with respect to the WS-cell free volume V, but keeping fixed the microion chemical potentials $\mu_\pm = \beta^{-1}\ln\left(n_{\rm b}\zeta_\pm^3\right)$,

$$\begin{aligned}\beta P_{\rm DH}^{\rm sgc}(\phi,n_{\rm b}) = -\left.\frac{{\rm d}\beta\Omega_{\rm DH}}{{\rm d}V}\right|_{Z,T,\mu_\pm} &= \frac{n_{\rm c}}{\eta}\left\{1+\frac{\eta^2}{2}(\eta^2-1) + \frac{Z\kappa\ell_B\eta^3}{4\Delta_2^2(\kappa R,\kappa a)}\left[\frac{\Delta_1(\kappa R,\kappa a)}{\kappa a}\times\right.\right.\\ &\left.\left.\times\,\left[\Delta_1(\kappa R,\kappa a)-\Delta_2(\kappa R,\kappa a)\right] - 4\kappa a\left(1+\frac{2\kappa^2a^2}{3\eta^2}-\kappa^2R^2\right) - 4\left(1-\frac{2}{3\eta^2}\right)\kappa^3R^3\right]\right\},\end{aligned} \tag{70}$$

where the prefactor of the right-hand side represents the ideal-gas Donnan osmotic pressure taking only the WS-cell charge neutrality (39) into account,

$$\frac{n_{\rm c}}{\eta} = \bar{n}_+ + \bar{n}_- = \sqrt{n_{\rm c}^2 + (2n_{\rm b})^2}. \tag{71}$$

In analogy to the salt-free, Eq. (32), and the canonical, Eq. (50), cases, the first term of (70) represents the ideal-gas law associated to the state-independent zero-th order Donnan densities, while the remaining terms correspond to the mean-field electrostatic corrections due to the microionic polarization around the polyion. We should note that the second term inside curly brackets depends only on η and is thus ℓ_B independent. This could suggest that the zero-th order Donnan ideal-gas law, $\lim_{\ell_B\to 0}\beta P_{\rm DH}^{\rm sgc} = n_{\rm c}/\eta$, would not be recovered in the weak-coupling limit. This ℓ_B-independent term, however, is indeed necessary to cancel the contributions that arise from the last term in the $\ell_B \to 0$ limit in order to give the correct potential-independent infinite-temperature limit. Moreover, it is shown in Appendix E that the linearized semi-grand-canonical osmotic pressure (70) corresponds to a quadratic expansion of the nonlinear semi-grand-canonical osmotic pressure (E5).

The linearized osmotic-pressure difference between the colloidal suspension and the infinite salt reservoir obeys $\beta\Delta P_{\rm DH} \equiv \beta P_{\rm DH}^{\rm sgc} - 2n_{\rm b} = \beta P_{\rm DH}^{\rm sgc} - (n_{\rm c}/\eta)\sqrt{1-\eta^2}$, with $\beta P_{\rm DH}^{\rm sgc}$ given by Eq. (70). In the next section we show that the linearized semi-grand-canonical osmotic-pressure difference $\beta\Delta P_{\rm DH}$ is intrinsically thermodynamically unstable in the infinite-dilution limit and we compare with expressions previously obtained by Deserno and von Grünberg.[65]

4 Comparison with Deserno and von Grünberg results

As already pointed out previously in the literature,[64,65] in this section we will show that the linearized semi-grand-canonical osmotic pressure $P_{\rm DH}^{\rm sgc}$ defined by Eq. (70) yields artifacts in the low-temperature, high-surface charge or infinite-dilution (of polyions) limits. In contradiction to the exact nonlinear result (E5), which yields an osmotic-pressure difference that is always positive,[88] $\beta\Delta P = \beta P - 2n_{\rm b} > 0$, the linearized

version $\Delta P_{\rm DH}$ becomes negative in the above mentioned limits. In an attempt to define the osmotic pressure in a linearized framework, Deserno and von Grünberg[65] introduced an alternative definition, P_1, that has the advantage of being exempt from any instabilities and is obtained via the *partial derivative* of the semi-grand-canonical potential with respect to the volume, keeping the optimal linearization point $\bar{\psi}_{\rm opt}$ (to be defined below) fixed. Their second osmotic pressure definition coincides with the linearized version (70) obtained in the previous section, $P_2 \equiv P_{\rm DH}^{\rm sgc}$, and is obtained via the *total derivative* of the semi-grand-canonical potential with respect to the volume. These two distinct osmotic-pressure definitions are given, respectively, by Eqs. (43) and (44) of Ref. [65] for $d = 3$,

$$\frac{\beta P_1}{2n_{\rm b}} = 1 + \frac{\left(\cosh\bar{\psi}_{\rm opt} - 1\right)^2}{2\cosh\bar{\psi}_{\rm opt}} + \frac{\sinh^2\bar{\psi}_{\rm opt}}{2\cosh\bar{\psi}_{\rm opt}}\left(\frac{1-\phi}{3\mathcal{D}\sqrt{\phi}}\right)^2 \geq 1, \tag{72}$$

$$\frac{\beta P_2}{2n_{\rm b}} = \frac{\beta P_1}{2n_{\rm b}} - \frac{\sinh^4\bar{\psi}_{\rm opt}}{2\cosh^3\bar{\psi}_{\rm opt}}\left\{\frac{1-\phi}{6\phi}\left[\frac{1}{\mathcal{D}^2} - \kappa a\frac{\mathcal{E}}{\mathcal{D}} + \kappa^2 a^2\left(1 - \frac{\mathcal{E}^2}{\mathcal{D}^2}\right)\right] - 1\right\}, \tag{73}$$

$$\mathcal{D} = I_{3/2}(\kappa R)\, K_{3/2}(\kappa a) - K_{3/2}(\kappa R)\, I_{3/2}(\kappa a), \tag{74}$$

$$\mathcal{E} = I_{3/2}(\kappa R)\, K_{1/2}(\kappa a) + K_{3/2}(\kappa R)\, I_{1/2}(\kappa a), \tag{75}$$

where $\{I_\nu, K_\nu\}$ are the modified Bessel functions[89] of the first and the second kind, respectively, and the optimal linearization point $\bar{\psi}_{\rm opt}$ satisfies the relations

$$\tanh\bar{\psi}_{\rm opt} = -\eta, \qquad \cosh\bar{\psi}_{\rm opt} = \left(\frac{\kappa}{\kappa_{\rm b}}\right)^2 = \frac{1}{\sqrt{1-\eta^2}}, \qquad \sinh\bar{\psi}_{\rm opt} = -\frac{n_{\rm c}}{2n_{\rm b}} = -\frac{\eta}{\sqrt{1-\eta^2}}. \tag{76}$$

In accordance with Eqs. (23) and (26) of Ref. [65], they can be recast in a simpler formal form in terms of the gauge-invariant electrostatic potential differences $\delta_\nu(\boldsymbol{r})$, defined by Eq. (62),

$$\beta P_1 = \frac{n_{\rm c}}{\eta}\left[1 - \frac{\eta^2}{2} + \frac{2Z^2\kappa^2\ell_B^2}{\Delta_2^2(\kappa R, \kappa a)}\right] = \frac{n_{\rm c}}{\eta}\left[1 + \eta\delta_1(R) + \frac{1}{2}\delta_2(R)\right], \tag{77}$$

$$\beta P_2 = \frac{n_{\rm c}}{\eta}\left[1 + \eta\delta_1(R) + \frac{1}{2}\delta_2(R) - \frac{\eta^2}{2}\left\langle\delta_2(\boldsymbol{r})\right\rangle\right], \tag{78}$$

from which one can see that they differ by a term that is quadratic in the electrostatic-potential difference. Looking at Eq. (C14) of Appendix C, one may trace back that the omitted contribution in P_1 originates from the volume dependence of the optimal linearization point $\bar{\psi}_{\rm opt}$, in accordance to the interpretation given by Deserno and von Grünberg[65] for the two distinct pressure definitions. We should recall that the linearized semi-grand-canonical osmotic-pressure (70) coincides with the second pressure definition, $P_{\rm DH}^{\rm sgc} \equiv P_2$, as shown in Appendix E by a quadratic expansion of the nonlinear osmotic pressure. It corresponds indeed to the negative *total derivative* of the linearized semi-grand-canonical potential $\Omega_{\rm DH}$ with respect to the WS-cell free volume V, which we thus believe to be the consistent and correct definition of the osmotic pressure.

It is convenient to introduce the dimensionless linearized osmotic-pressure differences,

$$\Pi_i \equiv \frac{\beta\Delta P_i}{2n_{\rm b}} = \frac{\beta P_i}{2n_{\rm b}} - 1, \qquad i = 1, 2. \tag{79}$$

In the vanishing volume fraction of polyions (infinite-dilution) limit, $\phi = (a/R)^3 \to 0$, we may write the asymptotic linearized osmotic-pressure differences in terms of $\theta \equiv 3Z\ell_B/a$ and $\hat{a} \equiv \kappa_{\rm b}a$,

$$\Pi_1 = \frac{\theta^4\phi^4}{8\hat{a}^8} + \mathscr{O}\left[\phi^5, \theta^2\phi^{2/3}\exp\left(-2\hat{a}\phi^{-1/3}\right)\right], \tag{80}$$

$$\Pi_2 = -\frac{\theta^4\phi^3}{12\hat{a}^5(1+\hat{a})^2} - \frac{5\theta^4\phi^4}{8\hat{a}^8}\left[\frac{2\hat{a}^3}{5\left(1+\hat{a}\right)^2} - 1\right] + \mathscr{O}\left[\phi^5, \theta^2\phi^{2/3}\exp\left(-2\hat{a}\phi^{-1/3}\right)\right], \tag{81}$$

which lead to the asymptotic linearized inverse isothermal compressibilities,

$$\beta\chi_1^{-1} \equiv 2n_{\rm b}n_{\rm p}\frac{{\rm d}\Pi_1}{{\rm d}n_{\rm p}} = \frac{Zn_{\rm p}\theta^3\phi^3}{2\hat{a}^6} + \mathscr{O}\left[\phi^4, \theta\phi^{-2/3}\exp\left(-2\hat{a}\phi^{-1/3}\right)\right], \tag{82}$$

$$\beta\chi_2^{-1} \equiv 2n_{\rm b}n_{\rm p}\frac{{\rm d}\Pi_2}{{\rm d}n_{\rm p}} = -Zn_{\rm p}\theta^3\left\{\frac{\phi^2}{4\hat{a}^3(1+\hat{a})^2}+\frac{5\phi^3}{2\hat{a}^6}\left[\frac{2\hat{a}^3}{5\left(1+\hat{a}\right)^2}-1\right]\right\}$$
$$+\mathscr{O}\left[\phi^4,\theta\phi^{-2/3}\exp\left(-2\hat{a}\phi^{-1/3}\right)\right]. \qquad (83)$$

While neglecting the contribution of the last quadratic term in the linearized osmotic pressure P_1 always leads to positive isothermal compressibilities, $\lim_{\phi\to 0}\chi_1 > 0$, its inclusion in P_2 *always* yields negative isothermal compressibilities in the infinite-dilution limit for nonvanishing ℓ_B, $\lim_{\phi\to 0}\chi_2 < 0$. This means that the pressure definition P_2 predicts that the infinite-dilution phase is unstable, in contrast to the canonical case, as shown in Figure 3. Therefore the *thermodynamically consistent* linearized osmotic pressure P_2 *intrinsically fails at infinite dilution,* leading to negative isothermal compressibilities in this limit. This fact was first noticed for the spherical case in Ref. [64] and generalized to WS cells in d-dimensions in Ref. [65]. For finite densities, in contrast to the canonical case (Figure 2), the low-ϕ dilute (gas) phase may only be stable for sufficiently small bulk salt concentrations, as shown in Figure 3. For sufficiently large $\kappa_{\rm b}a$ the finite-temperature critical point — located in the vicinity of the salt-free critical point (the black circle in Figure 3) — disappears. Note the nonmonotonic behaviour of the spinodal lines associated to P_2 for $\kappa_{\rm b}a = 10^{-1}$ and $\kappa_{\rm b}a = 10^2$ (inset), which leads to oscillating osmotic pressures. We should note, however, that the WS-cell model ceases to be meaningful for such high volume fractions in the latter case of strong screening. Finally we should remark that *beyond* the linearized PB WS-cell model approximation the thermodynamical instability at the infinite-dilution limit will be removed by taking into account the translational entropy of the polyions, which yields an osmotic-pressure contribution that is linear in ϕ and, therefore, overcomes the negative cubic leading term in the asymptotic linearized osmotic-pressure difference (81). However, because our analysis restricts to the linearization of the PB WS-cell model, the effect of this stabilizing entropic contribution — which may drastically alter the spinodal lines, specially in the low-volume fraction region — is not considered here. Note that the PB WS-cell model, in its full nonlinear version, is fully stable[82] even without invoking this stabilizing contribution.

Let us stress again that thermodynamic consistency and stability are independent concepts. This can be illustrated by inspecting the two linearized osmotic-pressure definitions proposed in Ref. [65]. The linearized osmotic pressure Π_2, although not fully stable, is self-consistent with quadratic expansions of the nonlinear osmotic pressure. The unstable region of Π_2 just reflects the breakdown of the linearization scheme to the nonlinear PB equation. On the other hand, Π_1, that displays positive isothermal compressibilities in the infinite-dilution limit and does not present any instabilities, is not *thermodynamically consistent,* its stability being purely fortuitous. This can be further fortified by comparing the *exact* analytical expressions of the nonlinear osmotic pressure for the planar geometry[27] with the two corresponding linearized versions. In the subsequent paper we show that both linearized expressions, Π_1 and Π_2, approach asymptotically the exact nonlinear result in the appropriate (weak-coupling, $\ell_B \to 0$) limit. Their convergence, however, are very different and it is the self-consistent definition Π_2 that gives a better approximation to the full nonlinear equation. Although analytical proofs can only be obtained for the planar case, we believe the same argument applies for any geometry.

5 Concluding remarks

We performed a linearization scheme consistent with quadratic expansions of the appropriate nonlinear thermodynamic functional. By using gauge-invariant forms of the electrostatic potential, we have shown that the linearized osmotic pressures correspond to quadratic expansions of the corresponding nonlinear versions for the three cases investigated: in the presence of neutralizing counterions only (salt-free case), in the presence of fixed amount of added salt (canonical case) and in electrochemical equilibrium with an infinite salt-reservoir (Donnan equilibrium, semi-grand-canonical case).

Contrary to previous works,[64,65] we adopted a gauge-invariant formulation with the inclusion of a Lagrange multiplier term to account for the charge-neutrality constraint. In the case of the Donnan equilibrium, it is shown that the minimization of the associated linearized semi-grand-canonical functional leads indeed to the state-independent zero-th order Donnan densities as the self-consistent expansion averages for the linearization. Therefore the optimality of the optimal expansion point $\bar{\psi}_{\rm opt}$ introduced by Deserno and von Grünberg[65] can be understood as corresponding to a self-consistent minimization of the linearized functional.

It is shown that the self-consistent linearized osmotic pressure in the semi-grand-canonical ensemble — as already pointed out in the literature[64,65] — leads to artifacts in the infinite-dilution, high-surface charge and strong-coupling limits, where it predicts negative osmotic-pressure differences between the colloidal suspension and the salt reservoir and negative isothermal compressibilities. Attempts to define a fully stable linearized equation of state based on the partial derivative of the linearized semi-grand-canonical potential with respect to the volume[65] can not be justified in our approach based on the minimization of the linearized functional, its stability being a fortuitous result. This can be seen most clearly in the analytically tractable case of two infinite charged planes in electrochemical equilibrium with an infinite salt reservoir, which we present in a companion paper.[27]

To avoid confusion we should stress at this point the exactness of the PB nonlinear solution at the mean-field level, its range of validity and limitations. In this work we discussed the linearization procedure in the framework of the nonlinear PB and the WS-cell model. The linearization constitutes here an approximation to the nonlinear treatment, whose exact results (at mean-field level) may be then compared to the linearized ones, allowing a control over the approximations and the onset of possible artifacts introduced by the linearization. Of course, we are not able to predict correct results for real systems when the (starting) nonlinear theory itself breaks down. In this case, an eventual linearized result may *accidentally* lead to a correct prediction of, say, phase separation, due to the simultaneous application of two inadequate approximations, namely, the mean-field PB equation and its subsequent linearization. The fact that PB nonlinear theory for WS-cell models always leads to stable suspensions does not invalidate phase separation in real systems, which may be due to finite-size effects, *intra- and intercell* microion-microion and *intercell* polyion-microion correlations that are neglected in the WS-cell mean-field PB picture. In the Donnan-equilibrium case, one should also take the microion-microion correlations in the infinite salt reservoir into account. However, the phase separation in deionized aqueous suspensions of charged colloids predicted by linearized theories[52,53,54,55,56,57,58,59] — which are claimed[52,53] to be driven by the state-independent volume terms[50,51] — seems to be related to mathematical artifacts of the linearization itself and does not correspond thus to a real physical effect, as already pointed out in previous works[64,65] via the linearization of the PB functional for WS-cell models and revisited it here.

Acknowledgments

The authors are grateful to M. Deserno and Y. Levin for thoughtful and intensive discussions, in particular to the former for sharing his results on the Donnan linearization prior to publication. Discussions with H. H. von Grünberg and E. Trizac are also acknowledged. We would also like to thank the financial support by the Max-Planck-Gesellschaft and the Alexander von Humboldt-Stiftung.

A Nonlinear osmotic-pressure boundary density theorem

In this Appendix it will be shown that the salt-free nonlinear osmotic pressure is related to the counterion density at the WS-cell boundary — see also Section 3 of Ref. [19] for the fixed-gauge derivation. For the Donnan problem, the fixed-gauge derivation is presented in Section II.C of Ref. [65].

The osmotic pressure (over the pure solvent) P is defined as the negative total derivative of the Helmholtz free energy F — the functional $\mathscr{F}$ evaluated at the equilibrium profile $n(\boldsymbol{r}) = \bar{n}(\boldsymbol{r})$ — with respect to the WS-cell free volume V,

$$P = -\frac{\mathrm{d}F}{\mathrm{d}V} = -\frac{\mathrm{d}\mathscr{F}[\bar{n}(\boldsymbol{r})]}{\mathrm{d}V}. \tag{A1}$$

The calculation of the osmotic pressure starting from the explicit form of the optimized Helmholtz free energy F, Eq. (16), turns out to be nontrivial, because both the equilibrium counterion profile $\bar{n}(\boldsymbol{r})$ as well as the Lagrange multiplier $\beta\bar{\mu}_{\mathrm{el}}$ depend implicitly on the WS-cell free volume V. However, because $\beta\mu_{\mathrm{el}}$ was introduced as a Lagrange multiplier to enforce the charge neutrality, it is much easier to consider the total derivative with respect to the volume of the extended Helmholtz free-energy *functional* $\tilde{\Omega}[n(\boldsymbol{r})] = \mathscr{F} - \mu_{\mathrm{el}} \int \mathrm{d}^3\boldsymbol{r}\, \rho(\boldsymbol{r})$ — but now considering the Lagrange multiplier μ_{el} *independent* of the WS-cell free volume

V — evaluated at the optimized profile $n(\boldsymbol{r}) = \bar{n}(\boldsymbol{r})$,

$$\frac{\mathrm{d}\mathscr{F}[\bar{n}(\boldsymbol{r})]}{\mathrm{d}V} = \left.\frac{\delta\tilde{\Omega}[n(\boldsymbol{r})]}{\delta V}\right|_{\bar{n}(\boldsymbol{r})} = \left.\frac{\partial\tilde{\Omega}[n(\boldsymbol{r})]}{\partial V}\right|_{\bar{n}(\boldsymbol{r})} + \int \mathrm{d}^3\boldsymbol{r}' \left.\frac{\delta\tilde{\Omega}[n(\boldsymbol{r})]}{\delta n(\boldsymbol{r}')}\right|_{\bar{n}(\boldsymbol{r}')} \frac{\mathrm{d}\bar{n}(\boldsymbol{r}')}{\mathrm{d}V}, \tag{A2}$$

where the derivatives of $\tilde{\Omega}$ are taken with constant μ_{el}. Because $\tilde{\Omega}[n(\boldsymbol{r})]$ is stationary with respect to the optimized profile $\bar{n}(\boldsymbol{r})$,

$$\left.\frac{\delta\tilde{\Omega}[n(\boldsymbol{r})]}{\delta n(\boldsymbol{r}')}\right|_{\bar{n}(\boldsymbol{r}')} = 0, \tag{A3}$$

only the partial-derivative term contributes to the osmotic pressure. Furthermore, because the only explicit dependence of $\tilde{\Omega}[n(\boldsymbol{r})]$ comes from the integration limit,[19] we are lead to

$$\begin{aligned}\beta P &= -\frac{\mathrm{d}\beta\mathscr{F}[\bar{n}(\boldsymbol{r})]}{\mathrm{d}V} = -\left.\frac{\partial\beta\tilde{\Omega}[n(\boldsymbol{r})]}{\partial V}\right|_{\bar{n}(\boldsymbol{r})} = -\left.\frac{\partial\beta\mathscr{F}[n(\boldsymbol{r})]}{\partial V}\right|_{\bar{n}(\boldsymbol{r})} + \left[\beta\mu_{\mathrm{el}}\frac{\partial}{\partial V}\int \mathrm{d}^3\boldsymbol{r}\, n(\boldsymbol{r})\right]_{\bar{n}(\boldsymbol{r})} \\ &= -\bar{\psi}(R)\bar{n}(R) - \bar{n}(R)\left\{\ln\left[\bar{n}(R)\zeta^3\right] - 1\right\} + \beta\bar{\mu}_{\mathrm{el}}\,\bar{n}(R) = \bar{n}(R),\end{aligned} \tag{A4}$$

which is the mean-field result[23] that relates the salt-free nonlinear osmotic pressure to the counterion density at the WS-cell boundary when intracell microion-microion correlations are neglected.

B Linearized free energy from a Debye charging process

In this Appendix it is shown that the linearized Helmholtz free energy can also be obtained by a Debye charging process[10] of the linearized electrostatic energy. This is obtained by inserting the DH-like solution (25) into (6),

$$\begin{aligned}\beta U(\kappa,\ell_B) &= \frac{1}{8\pi\ell_B}\int \mathrm{d}^3\boldsymbol{r}\,\left[\nabla\psi(r)\right]^2 \\ &= \frac{Z^2\ell_B}{2a\Delta_2^2(\kappa R,\kappa a)}\left[\Delta_1(\kappa R,\kappa a)\Delta_2(\kappa R,\kappa a) - \kappa^2 a\int_a^R \mathrm{d}r\,\Delta_1^2(\kappa R,\kappa r)\right].\end{aligned} \tag{B1}$$

The linearized excess Helmholtz free energy over the ideal-gas entropy of the reference uniform state is then obtained by a Debye charging process[10] of the linearized electrostatic energy (B1),

$$\beta F_{\mathrm{DH}} - Z\left[\ln\left(n_{\mathrm{c}}\zeta^3\right) - 1\right] = 2\int_0^1 \mathrm{d}\lambda\,\frac{\beta U(\lambda\kappa,\lambda^2\ell_B)}{\lambda} = \frac{Z^2\ell_B}{2a}\left[\frac{\Delta_1(\kappa R,\kappa a)}{\Delta_2(\kappa R,\kappa a)} - \frac{3a}{\kappa^2\left(R^3-a^3\right)}\right], \tag{B2}$$

which regains Eq. (31), obtained by adding the linearized electrostatic energy (B1) to the quadratic expansion of the ideal-gas entropy.

C Formal derivation of the linearized osmotic pressure

In this Appendix it will be shown that the salt-free linearized osmotic pressure is given by a quadratic expansion of the nonlinear counterion density at the WS-cell boundary,

$$\begin{aligned}\beta P_{\mathrm{DH}} &= -\frac{\mathrm{d}\beta F_{\mathrm{DH}}}{\mathrm{d}V} = -\frac{\mathrm{d}\beta\mathscr{F}_{\mathrm{DH}}[\bar{n}(\boldsymbol{r})]}{\mathrm{d}V} \\ &= n_{\mathrm{c}}\left\{1 + \langle\bar{\psi}\rangle - \bar{\psi}(R) + \frac{1}{2}\left[\langle\bar{\psi}\rangle - \bar{\psi}(R)\right]^2 - \frac{1}{2}\left\langle\left[\langle\bar{\psi}\rangle - \bar{\psi}\right]^2\right\rangle\right\},\end{aligned} \tag{C1}$$

which may be obtained by truncating the expansion of the salt-free nonlinear PB osmotic pressure up to the quadratic terms,

$$\beta P = \frac{n_{\mathrm{c}}\exp\left[\langle\bar{\psi}\rangle - \bar{\psi}(R)\right]}{\left\langle\exp\left[\langle\bar{\psi}\rangle - \bar{\psi}(\boldsymbol{r})\right]\right\rangle} = \beta P_{\mathrm{DH}} + \mathscr{O}\left(\left[\langle\bar{\psi}\rangle - \bar{\psi}(R)\right]^3, \left\langle\left[\langle\bar{\psi}\rangle - \bar{\psi}\right]^3\right\rangle\right), \tag{C2}$$

where the bar denotes equilibrium properties. One route to check that the salt-free linearized osmotic pressure (32) may be cast in the form (C1) is by using the linearized DH-like solution to the electrostatic potential (25) and computing explicitly the spatial averages

$$\left\langle \frac{\Delta_1(\kappa R,\kappa r)}{r} \right\rangle = \frac{4\pi}{V}\int_a^R \mathrm{d}r\, r\, \Delta_1(\kappa R,\kappa r) = -\frac{4\pi}{V}\left.\frac{\Delta_2(\kappa R,\kappa r)}{\kappa^2}\right|_a^R = \frac{\Delta_2(\kappa R,\kappa a)}{Z\ell_B}, \tag{C3}$$

$$\left\langle \frac{\Delta_1^2(\kappa R,\kappa r)}{r^2} \right\rangle = \frac{4\pi}{V}\int_a^R \mathrm{d}r\, \Delta_1^2(\kappa R,\kappa r) = -\frac{\kappa}{2Z\ell_B}\left\{\frac{\Delta_1(\kappa R,\kappa a)}{\kappa a}\times \right.$$
$$\left. \times\left[\Delta_1(\kappa R,\kappa a)-\Delta_2(\kappa R,\kappa a)\right] - 4\kappa a\left(1-\kappa^2R^2\right) - 4\kappa^3R^3\right\}. \tag{C4}$$

Alternatively, Eq. (C1) may be checked by taking a *formal* functional derivative with respect to the WS-cell free volume V — analogously as performed in Appendix A for the nonlinear treatment — of the salt-free linearized Helmholtz free energy functional (18), which is recast in the form

$$\beta\mathscr{F}_{\mathrm{DH}}[n(\boldsymbol{r})] = Z\left[\ln\left(n_{\mathrm{c}}\zeta^3\right)-1\right] + \int \mathrm{d}^3\boldsymbol{r}\, f[n(\boldsymbol{r})], \tag{C5}$$

$$f[n(\boldsymbol{r})] = \frac{1}{2}\psi(\boldsymbol{r})\rho(\boldsymbol{r}) + \frac{1}{2}n_{\mathrm{c}}\left[\frac{n(\boldsymbol{r})}{n_{\mathrm{c}}}-1\right]^2, \tag{C6}$$

where $\rho(\boldsymbol{r})$ and $\psi(\boldsymbol{r})$ are defined in Section 2 by Eqs. (2) and (4), respectively. The equilibrium counterion profile $\bar{n}(\boldsymbol{r})$ that minimizes the linearized version of the extended Helmholtz free-energy functional $\tilde{\Omega}_{\mathrm{DH}} = \mathscr{F}_{\mathrm{DH}} - \mu_{\mathrm{el}}\int \mathrm{d}^3\boldsymbol{r}\, n(\boldsymbol{r})$, with $\beta\bar{\mu}_{\mathrm{el}} = \langle\bar{\psi}\rangle$, is given by

$$\bar{n}(\boldsymbol{r}) = n_{\mathrm{c}}\left[1+\langle\bar{\psi}\rangle - \bar{\psi}(\boldsymbol{r})\right]. \tag{C7}$$

As explained in Appendix A for the nonlinear PB treatment, it is much easier to evaluate

$$\frac{\mathrm{d}\mathscr{F}_{\mathrm{DH}}[\bar{n}(\boldsymbol{r})]}{\mathrm{d}V} = \left.\frac{\delta\tilde{\Omega}_{\mathrm{DH}}[n(\boldsymbol{r})]}{\delta V}\right|_{\bar{n}(\boldsymbol{r})} = \left.\frac{\partial\tilde{\Omega}_{\mathrm{DH}}[n(\boldsymbol{r})]}{\partial V}\right|_{\bar{n}(\boldsymbol{r})} + \int \mathrm{d}^3\boldsymbol{r}'\left.\frac{\delta\tilde{\Omega}_{\mathrm{DH}}[n(\boldsymbol{r})]}{\delta n(\boldsymbol{r}')}\right|_{\bar{n}(\boldsymbol{r}')}\frac{\mathrm{d}\bar{n}(\boldsymbol{r}')}{\mathrm{d}V}, \tag{C8}$$

because the second term vanishes due to the stationary condition. The first term reads

$$-\frac{\partial\beta\tilde{\Omega}_{\mathrm{DH}}[n(\boldsymbol{r})]}{\partial V} = n_{\mathrm{c}} + \beta\mu_{\mathrm{el}}\frac{\partial}{\partial V}\int \mathrm{d}^3\boldsymbol{r}\, n(\boldsymbol{r}) - \frac{\partial}{\partial V}\int \mathrm{d}^3\boldsymbol{r}\, f[n(\boldsymbol{r})] - \frac{\mathrm{d}n_{\mathrm{c}}}{\mathrm{d}V}\int \mathrm{d}^3\boldsymbol{r}\,\frac{\partial f[n(\boldsymbol{r})]}{\partial n_{\mathrm{c}}}, \tag{C9}$$

$$\frac{\partial}{\partial V}\int \mathrm{d}^3\boldsymbol{r}\, f[n(\boldsymbol{r})] = \psi(R)n(R) + \frac{1}{2}n_{\mathrm{c}}\left[\frac{n(R)}{n_{\mathrm{c}}}-1\right]^2, \tag{C10}$$

$$\frac{\mathrm{d}n_{\mathrm{c}}}{\mathrm{d}V}\int \mathrm{d}^3\boldsymbol{r}\,\frac{\partial f[n(\boldsymbol{r})]}{\partial n_{\mathrm{c}}} = -\frac{n_{\mathrm{c}}}{V}\int \mathrm{d}^3\boldsymbol{r}\left\{\frac{1}{2}\left[\frac{n(\boldsymbol{r})}{n_{\mathrm{c}}}-1\right]^2 - \frac{n(\boldsymbol{r})}{n_{\mathrm{c}}}\left[\frac{n(\boldsymbol{r})}{n_{\mathrm{c}}}-1\right]\right\}. \tag{C11}$$

Using the explicit form (C7) of the linearized equilibrium counterion profile $\bar{n}(\boldsymbol{r})$, we obtain

$$\frac{\beta\bar{\mu}_{\mathrm{el}}}{n_{\mathrm{c}}}\frac{\partial}{\partial V}\int \mathrm{d}^3\boldsymbol{r}\, n(\boldsymbol{r})\Big|_{\bar{n}(\boldsymbol{r})} = \langle\bar{\psi}\rangle\left[1+\langle\bar{\psi}\rangle-\bar{\psi}(R)\right], \tag{C12}$$

$$\frac{1}{n_{\mathrm{c}}}\frac{\partial}{\partial V}\int \mathrm{d}^3\boldsymbol{r}\, f[n(\boldsymbol{r})]\Big|_{\bar{n}(\boldsymbol{r})} = \bar{\psi}(R)\left[1+\langle\bar{\psi}\rangle-\bar{\psi}(R)\right] + \frac{1}{2}\left[\langle\bar{\psi}\rangle-\bar{\psi}(R)\right]^2, \tag{C13}$$

$$\frac{1}{n_{\mathrm{c}}}\frac{\mathrm{d}n_{\mathrm{c}}}{\mathrm{d}V}\int \mathrm{d}^3\boldsymbol{r}\,\frac{\partial f[n(\boldsymbol{r})]}{\partial n_{\mathrm{c}}}\Big|_{\bar{n}(\boldsymbol{r})} = -\frac{1}{2}\left\langle\left[\langle\bar{\psi}\rangle-\bar{\psi}\right]^2\right\rangle + \left\langle\left[1+\langle\bar{\psi}\rangle-\bar{\psi}\right]\left[\langle\bar{\psi}\rangle-\bar{\psi}\right]\right\rangle$$
$$= \frac{1}{2}\left\langle\left[\langle\bar{\psi}\rangle-\bar{\psi}\right]^2\right\rangle, \tag{C14}$$

which yields the salt-free linearized osmotic pressure Eq. (C1).

D Linearized osmotic pressure: canonical ensemble

In this Appendix it will be shown that the linearized canonical osmotic pressure is given by a quadratic expansion of the nonlinear canonical osmotic pressure.

The nonlinear PB Helmholtz free-energy functional,

$$\beta\mathscr{F}[n_\pm(\boldsymbol{r})] = \frac{1}{8\pi\ell_B}\int \mathrm{d}^3\boldsymbol{r}\,\left[\nabla\psi(\boldsymbol{r})\right]^2 + \sum_{i=\pm}\int \mathrm{d}^3\boldsymbol{r}\, n_i(\boldsymbol{r})\left\{\ln\left[n_i(\boldsymbol{r})\zeta_i^3\right]-1\right\}, \tag{D1}$$

is minimized with respect to $n_\pm(\boldsymbol{r})$ under the constraint of overall WS-cell charge neutrality, Eq. (39). We introduce a Lagrange multiplier μ_{el} and define the extended Helmholtz free-energy functional, $\tilde{\Omega} = \mathscr{F} - \mu_{\mathrm{el}}\int \mathrm{d}^3\boldsymbol{r}\,\rho(\boldsymbol{r})$. Functional minimization of $\tilde{\Omega}$ with respect to $n_\pm(\boldsymbol{r})$ yields the Boltzmann factors, $n_\pm(\boldsymbol{r}) = \mathrm{e}^{\pm\beta\mu_{\mathrm{el}}\mp\psi(\boldsymbol{r})}/\zeta_\pm^3$. The Lagrange multiplier,

$$\beta\mu_{\mathrm{el}} = \ln\left(\bar{n}_+\zeta_+^3\right) - \ln\left\langle \mathrm{e}^{-\psi(\boldsymbol{r})}\right\rangle = \ln\left(\bar{n}_-\zeta_-^3\right) + \ln\left\langle \mathrm{e}^{\psi(\boldsymbol{r})}\right\rangle, \tag{D2}$$

is obtained by using the effective average definitions (34), which automatically satisfy the overall WS-cell charge neutrality, Eq. (39). Replacing into the Boltzmann factors, we obtain the nonlinear equilibrium density profiles,

$$n_\pm(\boldsymbol{r}) = \frac{\bar{n}_\pm\,\mathrm{e}^{\mp\psi(\boldsymbol{r})}}{\left\langle \mathrm{e}^{\mp\psi(\boldsymbol{r})}\right\rangle} = \frac{\bar{n}_\pm\exp\left[\pm\langle\psi\rangle\mp\psi(\boldsymbol{r})\right]}{\left\langle\exp\left[\pm\langle\psi\rangle\mp\psi(\boldsymbol{r})\right]\right\rangle}. \tag{D3}$$

The simple ideal-gas relation (17) between the nonlinear osmotic pressure and the WS-cell boundary density can be generalized in the presence of added salt. In this case, it can be shown that the nonlinear osmotic pressure is given by the total microionic density, $n \equiv n_+ + n_-$, evaluated at the WS-cell boundary,

$$\beta P = -\left.\frac{\mathrm{d}\beta F}{\mathrm{d}V}\right|_{Z,T,s} = n(R) = \frac{\bar{n}_+\,\mathrm{e}^{-\psi(R)}}{\left\langle \mathrm{e}^{-\psi(\boldsymbol{r})}\right\rangle} + \frac{\bar{n}_-\,\mathrm{e}^{\psi(R)}}{\left\langle \mathrm{e}^{\psi(\boldsymbol{r})}\right\rangle}. \tag{D4}$$

Let us now compare the linearized canonical osmotic pressure (50) with a quadratic expansion about the uniform reference state of its nonlinear counterpart, Eq. (D4),

$$\begin{aligned}\beta P &= (1+s)n_{\mathrm{c}}\frac{\exp\left[\langle\psi\rangle-\psi(R)\right]}{\left\langle\exp\left[\langle\psi\rangle-\psi(\boldsymbol{r})\right]\right\rangle} + sn_{\mathrm{c}}\frac{\exp\left[-\langle\psi\rangle+\psi(R)\right]}{\left\langle\exp\left[-\langle\psi\rangle+\psi(\boldsymbol{r})\right]\right\rangle}\\ &= (1+2s)n_{\mathrm{c}}\left\{1+\frac{1}{1+2s}\delta_1(R)+\frac{1}{2}\delta_2(R)-\frac{1}{2}\left\langle\delta_2(\boldsymbol{r})\right\rangle+\mathscr{O}\left[\delta_3(R),\left\langle\delta_3(\boldsymbol{r})\right\rangle\right]\right\},\end{aligned} \tag{D5}$$

where the electrostatic potential differences $\delta_\nu(\boldsymbol{r})$ are given by (62). Because of the redefinition of the screening length κ^{-1} in terms of κ_{c}^{-1}, the spatial averages (C3) and (C4) needed to evaluate $\langle\psi\rangle$ and $\left\langle\psi^2\right\rangle$ will be multiplied by a factor $(1+2s)^{-1}$. Using the explicit DH-like solution to the electrostatic potential (25), it is indeed possible to show that the linearized canonical osmotic pressure (50) corresponds to the truncation of the expansion (D5) up to the quadratic terms, i.e. $\beta P = \beta P_{\mathrm{DH}}^{\mathrm{can}} + \mathscr{O}\left[\delta_3(R),\left\langle\delta_3(\boldsymbol{r})\right\rangle\right]$, with $\beta P_{\mathrm{DH}}^{\mathrm{can}} = n_{\mathrm{DH}}(R) + (1+2s)\left(n_{\mathrm{c}}/2\right)\left[\delta_2(R)-\left\langle\delta_2(\boldsymbol{r})\right\rangle\right]$, where the first term corresponds to the sum of the *linearized* canonical densities at the WS-cell boundary. We see that the linearized canonical osmotic pressure *is not simply given* by the linearized boundary density $n_{\mathrm{DH}}(R)$, because of the presence of the quadratic terms.

E Linearized osmotic pressure: semi-grand-canonical ensemble

In this Appendix it will be shown that the linearized semi-grand-canonical osmotic pressure is given by a quadratic expansion of the nonlinear semi-grand-canonical osmotic pressure.

The nonlinear PB semi-grand-canonical functional associated to fixed microion chemical potentials $\beta\mu_\pm = \ln\left(n_{\mathrm{b}}\zeta_\pm^3\right)$,

$$\beta\Omega[n_\pm(\boldsymbol{r})] \equiv \beta\mathscr{F}[n_\pm(\boldsymbol{r})] - \sum_{i=\pm}\beta\mu_i\int \mathrm{d}^3\boldsymbol{r}\, n_i(\boldsymbol{r})$$

$$= \frac{1}{8\pi\ell_B}\int \mathrm{d}^3\boldsymbol{r}\,\left[\nabla\psi(\boldsymbol{r})\right]^2 + \sum_{i=\pm}\int \mathrm{d}^3\boldsymbol{r}\,n_i(\boldsymbol{r})\left\{\ln\left[\frac{n_i(\boldsymbol{r})}{n_\mathrm{b}}\right]-1\right\}, \tag{E1}$$

is minimized with respect to $n_\pm(\boldsymbol{r})$ under the constraint of overall WS-cell charge neutrality, Eq. (39). We introduce a Lagrange multiplier μ_el and define the extended semi-grand-canonical functional, $\tilde{\Omega} = \Omega - \mu_\mathrm{el}\int \mathrm{d}^3\boldsymbol{r}\,\rho(\boldsymbol{r})$. Functional minimization of $\tilde{\Omega}$ with respect to $n_\pm(\boldsymbol{r})$ yields the Boltzmann factors, $n_\pm(\boldsymbol{r}) = n_\mathrm{b}\mathrm{e}^{\pm\beta\mu_\mathrm{el}\mp\psi(\boldsymbol{r})}$. The Lagrange multiplier,

$$\mathrm{e}^{\pm\beta\mu_\mathrm{el}} = \frac{\sqrt{n_\mathrm{c}^2 + (2n_\mathrm{b})^2\left\langle \mathrm{e}^{\psi(\boldsymbol{r})}\right\rangle\left\langle \mathrm{e}^{-\psi(\boldsymbol{r})}\right\rangle} \pm n_\mathrm{c}}{2n_\mathrm{b}\left\langle \mathrm{e}^{\mp\psi(\boldsymbol{r})}\right\rangle}, \tag{E2}$$

is obtained by imposing the overall WS-cell charge neutrality, Eq. (39). Replacing into the Boltzmann factors, we obtain the nonlinear equilibrium density profiles,

$$n_\pm(\boldsymbol{r}) = \frac{\sqrt{n_\mathrm{c}^2 + (2n_\mathrm{b})^2\alpha_+\alpha_-} \pm n_\mathrm{c}}{2\alpha_\pm}\,\mathrm{e}^{\pm\langle\psi\rangle\mp\psi(\boldsymbol{r})} = \left[\bar{n}_\pm + \frac{1}{4}(1-\eta^2)\frac{n_\mathrm{c}}{\eta}\left\langle\delta_2(\boldsymbol{r})\right\rangle\right]\times$$
$$\times\left[1 \pm \delta_1(\boldsymbol{r}) + \frac{1}{2}\delta_2(\boldsymbol{r}) - \frac{1}{2}\left\langle\delta_2(\boldsymbol{r})\right\rangle\right] + \mathscr{O}\left[\delta_3(\boldsymbol{r}), \langle\delta_3(\boldsymbol{r})\rangle\right], \tag{E3}$$

$$\alpha_\pm = \left\langle \mathrm{e}^{\pm\langle\psi\rangle\mp\psi(\boldsymbol{r})}\right\rangle = 1 + \frac{1}{2}\left\langle\delta_2(\boldsymbol{r})\right\rangle + \mathscr{O}\left[\langle\delta_3(\boldsymbol{r})\rangle\right], \tag{E4}$$

where the electrostatic potential differences $\delta_\nu(\boldsymbol{r})$ are given by (62). At the nonlinear mean-field level the simple ideal-gas relation between the osmotic pressure and the total microionic density, $n \equiv n_+ + n_-$, at the WS-cell boundary is still valid, leading to

$$\beta P = -\left.\frac{\mathrm{d}\beta\Omega}{\mathrm{d}V}\right|_{Z,T,\mu_\pm} = n(R) = \frac{\sqrt{n_\mathrm{c}^2 + (2n_\mathrm{b})^2\alpha_+\alpha_-} + n_\mathrm{c}}{2\alpha_+}\,\mathrm{e}^{\langle\psi\rangle-\psi(R)} + \frac{\sqrt{n_\mathrm{c}^2 + (2n_\mathrm{b})^2\alpha_+\alpha_-} - n_\mathrm{c}}{2\alpha_-}\,\mathrm{e}^{-\langle\psi\rangle+\psi(R)}$$
$$= \frac{n_\mathrm{c}}{\eta}\left\{1 + \eta\delta_1(R) + \frac{1}{2}\delta_2(R) - \frac{\eta^2}{2}\left\langle\delta_2(\boldsymbol{r})\right\rangle + \mathscr{O}\left[\delta_3(R), \langle\delta_3(\boldsymbol{r})\rangle\right]\right\}. \tag{E5}$$

Let us again compare the linearized semi-grand-canonical osmotic pressure (70) with a quadratic expansion about the zero-th order Donnan densities $\bar{n}_\pm$, Eqs. (60), of its nonlinear counterpart, Eq. (E5). Now, because of the redefinition of κ, the spatial averages (C3) and (C4) needed to evaluate $\langle\psi\rangle$ and $\left\langle\psi^2\right\rangle$ are multiplied by a factor η. Using again the explicit DH solution (25), it is possible to show that the linearized semi-grand-canonical osmotic pressure (70) corresponds to the truncation of the expansion (E5) up to the quadratic terms, i.e. $\beta P = \beta P_\mathrm{DH}^\mathrm{sgc} + \mathscr{O}\left[\delta_3(R), \langle\delta_3(\boldsymbol{r})\rangle\right]$, with $\beta P_\mathrm{DH}^\mathrm{sgc} = n_\mathrm{DH}(R) + \left[n_\mathrm{c}/(2\eta)\right]\left[\delta_2(R) - \eta^2\left\langle\delta_2(\boldsymbol{r})\right\rangle\right]$, where the first term represents the sum of the *linearized* semi-grand-canonical densities at the WS-cell boundary. We see again that the linearized semi-grand-canonical osmotic pressure *does not correspond* to the linearized boundary density $n_\mathrm{DH}(R)$, because of the presence of the quadratic terms.

F Linearized averaged densities for the semi-grand-canonical ensemble

In this Appendix it will be shown that the self-consistent linearized averaged densities for the semi-grand-canonical ensemble are given by the state-independent zero-th order Donnan densities, which are obtained by a self-consistent minimization of the linearized semi-grand-canonical functional under the WS-cell charge-neutrality constraint.

To obtain the self-consistent averaged densities *up to second order* we need to expand the nonlinear semi-grand-canonical functional, Eq. (E1), *up to third order* about the (*a priori* unknown) effective average densities $\langle n_\pm(\boldsymbol{r})\rangle \equiv (1/V)\int \mathrm{d}^3\boldsymbol{r}\,n_\pm(\boldsymbol{r})$,

$$\beta\Omega[n_\pm(\boldsymbol{r})] = \frac{1}{8\pi\ell_B}\int \mathrm{d}^3\boldsymbol{r}\,\left[\nabla\psi(\boldsymbol{r})\right]^2 + V\sum_{i=\pm}\langle n_i\rangle\left[\ln\frac{\langle n_i\rangle}{n_\mathrm{b}} - 1\right] + \sum_{i=\pm}\left[\langle n_i\rangle\ln\langle n_i\rangle\right]\int \mathrm{d}^3\boldsymbol{r}\,\delta_i(\boldsymbol{r})$$
$$+\frac{1}{2}\sum_{i=\pm}\langle n_i\rangle\int \mathrm{d}^3\boldsymbol{r}\,\delta_i^2(\boldsymbol{r}) - \frac{1}{6}\sum_{i=\pm}\langle n_i\rangle\int \mathrm{d}^3\boldsymbol{r}\,\delta_i^3(\boldsymbol{r}) + \mathscr{O}\left[\int \mathrm{d}^3\boldsymbol{r}\,\delta_i^4(\boldsymbol{r})\right], \tag{F1}$$

where we introduced the relative deviations about the averaged densities,

$$\delta_{\pm}(\boldsymbol{r}) \equiv \frac{n_{\pm}(\boldsymbol{r})}{\langle n_{\pm}\rangle} - 1. \tag{F2}$$

Keeping only quadratic terms in Eq. (F1) is similar in spirit to the quadratic expansion presented in Eq. (13) of Ref. [65]. However, we want to stress that, in general, the unknown average expansion densities $\langle n_{\pm}\rangle$ depend itself on the ionic profiles. Functional minimization of Eq. (F1) with respect to the profiles $n_{\pm}(\boldsymbol{r})$ must take this fact into account, in addition to the WS-cell charge-neutrality constraint, Eq. (39). Eventually, for a linearized theory, the self-consistent expansion densities $\bar{n}_{\pm}$ turn out to be indeed independent on the ionic profiles, cf. Eq. (60), but this can only be derived *a posteriori*.

We introduce a Lagrange multiplier $\mu_{\rm el}$ to ensure the overall WS-cell charge neutrality (39), and define the extended semi-grand-canonical functional, $\tilde{\Omega} = \Omega - \mu_{\rm el}\int \mathrm{d}^3\boldsymbol{r}\,\rho(\boldsymbol{r})$. Functional minimization of $\tilde{\Omega}$ with respect to $n_{\pm}(\boldsymbol{r})$ leads to the Euler-Lagrange or stationary conditions, $\delta\tilde{\Omega}/\delta n_{\pm}(\boldsymbol{r}) = 0$, which may be cast in the form

$$n_{\pm}(\boldsymbol{r}) = \langle n_{\pm}\rangle \left\{ 1 \mp [\psi(\boldsymbol{r}) - \beta\mu_{\rm el}] - \ln\frac{\langle n_{\pm}\rangle}{n_{\rm b}} + \frac{1}{2}\delta_{\pm}^2(\boldsymbol{r}) + \mathscr{O}\left[\delta_{\pm}^3(\boldsymbol{r}), \langle\delta_{\pm}^3(\boldsymbol{r})\rangle\right] \right\}, \tag{F3}$$

where we have neglected the cubic averaged contribution, $\mathscr{O}\left[\langle\delta_{\pm}^3(\boldsymbol{r})\rangle\right]$, because the neglected quartic term of (F1) will also contributed to it. To obtain the averages $\langle n_{\pm}\rangle$ self-consistently, we integrate $n_{\pm}(\boldsymbol{r})$ over the volume to obtain the consistency relations,

$$\langle n_{\pm}(\boldsymbol{r})\rangle = n_{\rm b}\exp\left\{ \mp [\langle\psi(\boldsymbol{r})\rangle - \beta\mu_{\rm el}] + \frac{1}{2}\langle\delta_{\pm}^2(\boldsymbol{r})\rangle + \mathscr{O}\left[\langle\delta_{\pm}^3(\boldsymbol{r})\rangle\right] \right\}, \tag{F4}$$

where the Lagrange multiplier $\mu_{\rm el}$ is found by imposing the overall WS-cell charge neutrality (39). We should stress that in addition to the chemical potential of microions μ that defines the semi-grand-canonical ensemble, we introduced a *Lagrange multiplier* $\mu_{\rm el}$, whose role is twofold: besides the overall WS-cell charge neutrality (39), it also ensures the gauge invariance of the electrostatic potential $\psi(\boldsymbol{r})$. We should not confuse the chemical potential of microions μ, which is fixed by the bulk salt concentration $n_{\rm b}$ of the reservoir, with the linearized Lagrange multiplier $\mu_{\rm el}$, which is associated with the Donnan effect and ensures the charge neutrality of the WS cell (39).

Before we derive the averages consistent with a *linearization* of the PB equation, let us also obtain the self-consistent averages corresponding to a *quadratic approximation* of the nonlinear equation. Noting that $\delta_{\pm}(\boldsymbol{r}) = \pm\delta_1(\boldsymbol{r}) + \mathscr{O}\left[\delta_2(\boldsymbol{r}), \langle\delta_2(\boldsymbol{r})\rangle\right]$ and neglecting cubic terms in Eqs. (F3) and (F4) leads to the quadratic self-consistent averages,

$$\langle n_{\pm}(\boldsymbol{r})\rangle = \frac{\sqrt{n_{\rm c}^2 + (2n_{\rm b})^2 \mathrm{e}^{\langle\delta_2(\boldsymbol{r})\rangle}} \pm n_{\rm c}}{2}, \tag{F5}$$

and the quadratic equilibrium density profiles,

$$n_{\pm}(\boldsymbol{r}) = \langle n_{\pm}(\boldsymbol{r})\rangle \left[1 \pm \delta_1(\boldsymbol{r}) + \frac{1}{2}\delta_2(\boldsymbol{r}) - \frac{1}{2}\langle\delta_2(\boldsymbol{r})\rangle \right], \tag{F6}$$

where the electrostatic potential ν-th order difference $\delta_{\nu}(\boldsymbol{r})$ is defined by (62). These correspond indeed to the *quadratic* expansions of the nonlinear PB average densities and equilibrium density profiles, respectively, and are correct up to $\delta_2(\boldsymbol{r})$ (quadratic) terms. Here we may see another advantage of the gauge-invariant formulation: it provides us a systematic way to consider self-consistent higher-order approximations of the nonlinear equations, while the fixed-gauge analysis of Deserno and von Grünberg[65] does not allow them to extend their calculations to include higher-order terms.

However, in order to be consistent with a *linearization* of the PB equation one needs to neglect also the quadratic terms in the approximate Euler-Lagrange conditions (F3), although *global* self-consistency of the Legendre transformation will require to include them — cf. Appendix G. It is clear that ignoring these terms will yield the *state-independent* zero-th order Donnan densities as the self-consistent linearized averaged densities,

$$\langle n_{\pm}(\boldsymbol{r})\rangle = \frac{\sqrt{n_{\rm c}^2 + (2n_{\rm b})^2} \pm n_{\rm c}}{2}, \tag{F7}$$

and the linearized equilibrium density profiles,

$$n_{\pm}(\boldsymbol{r}) = \langle n_{\pm}(\boldsymbol{r})\rangle \left[1 \pm \delta_1(\boldsymbol{r})\right]. \tag{F8}$$

In the main text we used the notation $\bar{n}_{\pm} \equiv \langle n_{\pm}\rangle_1$, Eq. (60), to refer to the linearized self-consistent averaged densities for the semi-grand-canonical ensemble, where the subscript '1' emphasizes the fact that the average densities were obtained under linearization. Deserno and von Grünberg[65] justify this choice for the expansion densities — written in terms of an optimal linearization point $\bar{\psi}_{\rm opt}$ defined by $\bar{n}_{\pm} = n_{\rm b}{\rm e}^{\mp\bar{\psi}_{\rm opt}}$ — by arguing that any other choice for the linearization point would lead to conflicting inequalities involving nonlinear and linearized averages. In a gauge-invariant formulation, however, the justification is indeed based on the self-consistent *minimization* of the linearized semi-grand-canonical functional $\Omega_{\rm DH}[n_{\pm}(\boldsymbol{r})]$, which is obtained by truncating the expansion of the nonlinear functional $\Omega[n_{\pm}(\boldsymbol{r})]$, given by Eq. (F1), only up to the quadratic terms and neglecting (consistently under linearization) the quadratic contribution in the approximated averaged Euler-Lagrange equations, Eq. (F4). Although *internal* self-consistency (within the semi-grand-canonical ensemble) is achieved by using the linearized self-consistent averaged densities (60), we show in Appendix G that *global* self-consistency under linearization (between the canonical and the semi-grand-canonical ensembles) will also require the inclusion of the quadratic state-dependent terms of the self-consistent averaged densities (F5).

G Legendre transformation at the linearized level

In this Appendix we discuss the differences between the Legendre transformation connecting the canonical and the semi-grand-canonical ensembles at the level of the linearized functionals (before the functional minimization) and of the linearized thermodynamic potentials (after the functional minimization). It is shown that, in order to preserve the exactness of the Legendre transformation, quadratic contributions to the linearized expansion densities should be included in the former case, which are automatically included in the latter case.

At the nonlinear PB level the osmotic pressures obtained in the two distinct (canonical and semi-grand-canonical) ensembles are completely equivalent,[90] provided we map them using the nonlinear relation

$$(n_{\rm c}+n_{\rm s})n_{\rm s} = \langle n_+(\boldsymbol{r})\rangle \langle n_-(\boldsymbol{r})\rangle = n_{\rm b}^2 \left\langle {\rm e}^{\psi(\boldsymbol{r})}\right\rangle \left\langle {\rm e}^{-\psi(\boldsymbol{r})}\right\rangle, \tag{G1}$$

where $n_{\rm s} \equiv \langle n_-(\boldsymbol{r})\rangle$ is the effective average salt concentration in the colloidal suspension. The exact (at the mean-field level) relation (G1) follows directly from the gauge-invariant forms of the nonlinear average densities (61). Therefore, up to quadratic order, the linearized osmotic pressures are related by the renormalization of the total average density of microions in the two ensembles,

$$n \equiv n_{\rm c} + 2n_{\rm s} = (1+2s)\, n_{\rm c} \to \langle n_+(\boldsymbol{r})\rangle + \langle n_-(\boldsymbol{r})\rangle = \frac{n_{\rm c}}{\eta}\left\{1 + \frac{1}{2}\left(1-\eta^2\right)\langle \delta_2(\boldsymbol{r})\rangle + \mathscr{O}\left[\langle \delta_3(\boldsymbol{r})\rangle\right]\right\}. \tag{G2}$$

Because of the quadratic contribution, the linearized osmotic pressures obtained in the two ensembles *do not have the same form* when they are mapped using the zero-th order renormalization $(1+2s)\to\eta^{-1}$. In other words, although for the nonlinear equations the Legendre transformation between the canonical and the semi-grand-canonical ensembles is exact, the same does not hold for the linearized equations: one needs to use the approximated mapping (G2) and expand consistently the linearized osmotic pressure up to quadratic-order terms. This introduces an additional source of deviations for the linearized semi-grand-canonical equations of state. In particular, the thermodynamically-conjugated density (in the semi-grand-canonical ensemble) to the chemical potential of salt particles, $\mu_{\rm s} = \mu_+ + \mu_-$, with $\mu_{\pm} = \beta^{-1}\ln\left(n_{\rm b}\zeta_{\pm}^3\right)$, that corresponds to the (effective) total average density of microions inside the colloidal suspension, $n = \bar{n}_+ + \bar{n}_-$,

$$\begin{aligned} n \equiv -\frac{2{\rm d}}{{\rm d}\mu_{\rm s}}\left[\frac{\Omega_{\rm DH}}{V}\right]_{n_{\rm p}} = \frac{n_{\rm c}}{\eta}\left\{1 + \frac{\eta^2}{2}\left(\eta^2-1\right) + \frac{Z\kappa\ell_B\eta}{4\Delta_2^2(\kappa R,\kappa a)}\left(\eta^2-1\right)\times\right. \\ \left.\times\left[\frac{\Delta_1(\kappa R,\kappa a)}{\kappa a}\left[\Delta_1(\kappa R,\kappa a)-\Delta_2(\kappa R,\kappa a)\right] - 4\kappa a\left(1-\kappa^2R^2\right) - 4\kappa^3R^3\right]\right\}, \end{aligned} \tag{G3}$$

is indeed given by the right-hand side of Eq. (G2) neglecting cubic and higher-order contributions. This conjugated density, however, is *inconsistent* (up to the quadratic order, but consistent under *linearization*) with the state-independent zero-th order Donnan densities (60), i.e. $n \neq \bar{n}_+ + \bar{n}_- = n_{\rm c}/\eta$, because of the presence of the quadratic contribution in Eq. (G2).

An alternative procedure to the Legendre transformation of the linearized Helmholtz free-energy *functional* $\mathscr{F}_{\rm DH}[n_\pm(\boldsymbol{r})]$ — which is done, as presented in Appendix F, *before* the functional minimization with respect to the profiles — is to perform it *after* the functional minimization, at the Helmholtz *free-energy* level. Because in the canonical ensemble the expansion densities $\bar{n}_\pm$ are known *a priori*, the Legendre transformation that maps the linearized Helmholtz free energy $F_{\rm DH}$ into the linearized semi-grand-canonical potential $\Omega_{\rm DH}$ can then be obtained without any further approximations for the expansion densities. For this purpose it is convenient to recall the definition of the *total* volume of the WS cell and of the *nominal* densities of counterions, polyions and salt particles,

$$\tilde{V} \equiv \frac{V}{1-\phi}, \qquad \tilde{n}_{\rm c} \equiv n_{\rm c}\,(1-\phi)\,, \qquad n_{\rm p} \equiv \frac{1}{\tilde{V}} = \phi\left(\frac{4\pi}{3}a^3\right)^{-1}, \qquad \tilde{n}_{\rm s} \equiv n_{\rm s}\,(1-\phi)\,. \tag{G4}$$

It is important to stress that the *nominal* densities should be used, instead of the *effective* ones. Introducing the linearized Helmholtz free-energy density, $f_{\rm DH} \equiv F_{\rm DH}/\tilde{V}$, where $F_{\rm DH}$ in the presence of added salt is given by Eq. (46), one may check that the Legendre transformation at the linearized free-energy level is indeed *exact,* since the linearized chemical potentials of salt particles and of polyions,

$$\begin{aligned}
\beta\mu_{\rm s} \equiv\ & \left.\frac{{\rm d}\beta f_{\rm DH}}{{\rm d}\tilde{n}_{\rm s}}\right|_{n_{\rm p}} = \ln\left[(1+s)n_{\rm c}\zeta_+^3\right] + \ln\left(sn_{\rm c}\zeta_-^3\right) + \frac{1}{(1+2s)^2} + \frac{1}{1+2s}\,\frac{Z\kappa\ell_B}{2\Delta_2^2(\kappa R,\kappa a)}\times \\
& \times\left[\frac{\Delta_1(\kappa R,\kappa a)}{\kappa a}\left[\Delta_1(\kappa R,\kappa a)-\Delta_2(\kappa R,\kappa a)\right] - 4\kappa a\left(1-\kappa^2R^2\right) - 4\kappa^3R^3\right], \qquad \text{(G5)} \\
\beta\mu_{\rm p} \equiv\ & \left.\frac{{\rm d}\beta f_{\rm DH}}{{\rm d}n_{\rm p}}\right|_{\tilde{n}_{\rm s}} = n_{\rm p}^{-1}\left\{\tilde{n}_{\rm c}\ln\left[(1+s)n_{\rm c}\zeta_+^3\right] + \frac{\tilde{n}_{\rm c}}{2}\left[\frac{Z\ell_B}{a}\,\frac{\Delta_1(\kappa R,\kappa a)}{\Delta_2(\kappa R,\kappa a)} - \frac{1}{1+2s}\right] - \frac{s\tilde{n}_{\rm c}}{(1+2s)^2}\right. \\
& +(1+2s)n_{\rm c}\left[\phi + \frac{2Z^2\kappa^2\ell_B^2}{\Delta_2^2(\kappa R,\kappa a)}\right] + \frac{(1+2s\phi)\,n_{\rm c}}{1+2s}\,\frac{Z\kappa\ell_B}{4\Delta_2^2(\kappa R,\kappa a)}\times \\
& \left.\times\left[\frac{\Delta_1(\kappa R,\kappa a)}{\kappa a}\left[\Delta_1(\kappa R,\kappa a)-\Delta_2(\kappa R,\kappa a)\right] - 4\kappa a\left(1-\kappa^2R^2\right) - 4\kappa^3R^3\right]\right\}, \qquad \text{(G6)}
\end{aligned}$$

satisfy the thermodynamical identity

$$P_{\rm DH}^{\rm can} = \tilde{n}_{\rm s}\mu_{\rm s} + n_{\rm p}\mu_{\rm p} - f_{\rm DH}, \tag{G7}$$

where the linearized *canonical* osmotic pressure entering into Eq. (G7), $P_{\rm DH}^{\rm can}$, is given by Eq. (50). It should also be remarked that Eq. (G5) corresponds to the truncation of the expansion of the exact nonlinear mapping (G1) up to quadratic-order terms,

$$\beta\mu_{\rm s} = \ln\left[\frac{(n_{\rm c}+n_{\rm s})n_{\rm s}\zeta_+^3\zeta_-^3}{\left\langle {\rm e}^{\psi(\boldsymbol{r})}\right\rangle\left\langle {\rm e}^{-\psi(\boldsymbol{r})}\right\rangle}\right] = \ln\left[(1+s)n_{\rm c}\zeta_+^3\right] + \ln\left(sn_{\rm c}\zeta_-^3\right) - \langle\delta_2(\boldsymbol{r})\rangle + \mathscr{O}\left[\langle\delta_3(\boldsymbol{r})\rangle\right]. \tag{G8}$$

The thermodynamical relation (G7) can also be viewed as defining the Legendre transformation. Instead of obtaining the osmotic-pressure isotherms for a constant number of salt particles inside the WS cell (canonical case, fixed s), we may consider them at fixed chemical potential of salt particles $\mu_{\rm s}$ (semi-grand-canonical case), which corresponds to a system in electrochemical equilibrium with an infinite salt reservoir of bulk density $n_{\rm b}$, defined by

$$\beta\mu_{\rm s} \equiv \beta\mu_+ + \beta\mu_- = \ln\left(n_{\rm b}^2\zeta_+^3\zeta_-^3\right). \tag{G9}$$

Solution of the nonlinear equation defined by (G5) and (G9) yields the Legendre transformation in an implicit parametric form,

$$s(\phi,n_{\rm b}) = \frac{\sqrt{1+\left[2n_{\rm b}/n_{\rm c}(\phi)\right]^2{\rm e}^{\langle\delta_2(\boldsymbol{r})\rangle}}-1}{2}, \qquad n_{\rm c}(\phi) = \frac{3Z}{4\pi a^3}\left(\frac{\phi}{1-\phi}\right), \tag{G10}$$

with the quadratic electrostatic-potential deviation in the canonical ensemble given by

$$\langle\delta_2(\boldsymbol{r})\rangle \,=\, -\frac{1}{(1+2s)^2} - \frac{1}{1+2s}\,\frac{Z\kappa\ell_B}{2\Delta_2^2(\kappa R,\kappa a)}\,\times \\ \times\left[\frac{\Delta_1(\kappa R,\kappa a)}{\kappa a}\left[\Delta_1(\kappa R,\kappa a)-\Delta_2(\kappa R,\kappa a)\right]-4\kappa a\left(1-\kappa^2R^2\right)-4\kappa^3R^3\right]. \tag{G11}$$

The linearized *semi-grand-canonical* osmotic pressure, $\hat{P}^{\rm sgc}_{\rm DH}=\hat{P}^{\rm sgc}_{\rm DH}(\phi,n_{\rm b})$, is then obtained by inserting the Legendre transformation $s=s(\phi,n_{\rm b})$ into the linearized *canonical* osmotic pressure $P^{\rm can}_{\rm DH}=P^{\rm can}_{\rm DH}(\phi,s)$, Eq. (50). In other words, the two linearized osmotic pressures are related by $\hat{P}^{\rm sgc}_{\rm DH}(\phi,n_{\rm b})\equiv P^{\rm can}_{\rm DH}\left[\phi,s(\phi,n_{\rm b})\right]$. We should remark that the linearized semi-grand-canonical osmotic pressure obtained by this procedure, $\hat{P}^{\rm sgc}_{\rm DH}(\phi,n_{\rm b})$, *does not* coincide with its counterpart $P^{\rm sgc}_{\rm DH}(\phi,n_{\rm b})$ given by Eq. (70).

The disagreement between the two distinct linearized semi-grand-canonical osmotic pressures, $\hat{P}^{\rm sgc}_{\rm DH}(\phi,n_{\rm b})\neq P^{\rm sgc}_{\rm DH}(\phi,n_{\rm b})$ — obtained by Legendre transformations performed pre- and pos-minimization of the linearized functional $\mathscr{F}_{\rm DH}[n_\pm(\boldsymbol{r})]$ with respect to the profiles — may be traced back to the neglected quadratic contribution in the self-consistent linearized averaged densities (60). Although the neglect of this state-dependent contribution in the average densities (F5) is justified to ensure mathematical consistency of the truncation under the linearized approximation, in order to obtain *global* thermodynamic self-consistency (i.e., in order to preserve the *exactness*) of the Legendre transformation one needs to keep *all terms* of the quadratic truncation of the Euler-Lagrange equations, regardless of its inconsistency from the mathematical point of view. This leads to the average densities (F5), which include the quadratic state-dependent contribution $\langle\delta_2(\boldsymbol{r})\rangle$ — in contrast to Eqs. (60), which neglect it. Compared to the linearized semi-grand-canonical potential $\Omega_{\rm DH}$, Eq. (69), which uses the state-independent zero-th order Donnan densities (60) as expansion densities, an augmented version $\hat{\Omega}_{\rm DH}$ using the quadratic average densities (F5) will have an additional quadratic state-dependent contribution,

$$\beta\hat{\Omega}_{\rm DH} \,=\, Z\left[\operatorname{arctanh}\hat{\eta}-\frac{1}{\hat{\eta}}-\frac{\hat{\eta}}{2}+\frac{Z\ell_B}{2a}\,\frac{\Delta_1(\hat{\kappa}R,\hat{\kappa}a)}{\Delta_2(\hat{\kappa}R,\hat{\kappa}a)}+\frac{1}{2\hat{\eta}}\,\langle\delta_2(\boldsymbol{r})\rangle\right], \tag{G12}$$

where the parameter $\hat{\eta}$ and the (effective) Debye screening length $\hat{\kappa}^{-1}$ in the suspension,

$$\hat{\eta}\equiv\frac{n_{\rm c}}{\sqrt{n_{\rm c}^2+(2n_{\rm b})^2{\rm e}^{\langle\delta_2(\boldsymbol{r})\rangle}}},\qquad\qquad \hat{\kappa}^2=\frac{\kappa_{\rm c}^2}{\hat{\eta}}=\frac{\kappa_{\rm b}^2{\rm e}^{\langle\delta_2(\boldsymbol{r})\rangle/2}}{\sqrt{1-\hat{\eta}^2}}, \tag{G13}$$

are now given implicitly in terms of the quadratic electrostatic-potential deviation in the *semi-grand-canonical* ensemble, which is obtained by replacing $(1+2s)\to\hat{\eta}^{-1}$ and $\kappa\to\hat{\kappa}$ in the expression of its canonical counterpart, Eq. (G11). These yield the *globally* self-consistent (i.e., that preserve the exactness of the Legendre transformation) linearized semi-grand-canonical equations of state,

$$\hat{n} \,\equiv\, -\frac{2{\rm d}}{{\rm d}\mu_{\rm s}}\left[\frac{\hat{\Omega}_{\rm DH}}{V}\right]_{n_{\rm p}} = \frac{n_{\rm c}}{\hat{\eta}} = \sqrt{n_{\rm c}^2+(2n_{\rm b})^2{\rm e}^{\langle\delta_2(\boldsymbol{r})\rangle}} = \langle n_+(\boldsymbol{r})\rangle+\langle n_-(\boldsymbol{r})\rangle\,, \tag{G14}$$

$$\beta\hat{P}^{\rm sgc}_{\rm DH} \,\equiv\, -\left.\frac{{\rm d}\beta\hat{\Omega}_{\rm DH}}{{\rm d}V}\right|_{Z,T,\mu_\pm} = \frac{n_{\rm c}}{\hat{\eta}}\left\{1+\frac{Z\hat{\kappa}\ell_B\hat{\eta}}{4\Delta_2^2(\hat{\kappa}R,\hat{\kappa}a)}\left[\frac{\Delta_1(\hat{\kappa}R,\hat{\kappa}a)}{\hat{\kappa}a}\,\times\right.\right. \\ \left.\left.\times\,\left[\Delta_1(\hat{\kappa}R,\hat{\kappa}a)-\Delta_2(\hat{\kappa}R,\hat{\kappa}a)\right]-4\hat{\kappa}a\left(1+\frac{2}{3}\hat{\kappa}^2a^2-\hat{\kappa}^2R^2\right)-\frac{4}{3}\hat{\kappa}^3R^3\right]\right\}, \tag{G15}$$

where the total derivatives must take the $\langle\delta_2(\boldsymbol{r})\rangle$ parametric implicit dependence of Eqs. (G13) into account. The (effective) total average density of microions $\hat{n}$, Eq. (G14), the linearized semi-grand-canonical osmotic pressure $\hat{P}^{\rm sgc}_{\rm DH}$, Eq. (G15), and the linearized chemical potential of polyions $\mu_{\rm p}(\phi,n_{\rm b})$ are now fully consistent with their canonical counterparts, given respectively by $n=(1+2s)n_{\rm c}$ and Eqs. (50) and (G6). They are related by the Legendre transformation $(1+2s)=\hat{\eta}^{-1}$, where $\hat{\eta}$ — given implicitly by Eq. (G13) — also includes quadratic state-dependent contributions. A further Legendre transformation of the linearized semi-grand-canonical potential $\hat{\Omega}_{\rm DH}$ regains, as it should, the linearized pressure $\hat{P}^{\rm sgc}_{\rm DH}$,

$$\hat{P}^{\rm sgc}_{\rm DH}=n_{\rm p}\mu_{\rm p}-\frac{\hat{\Omega}_{\rm DH}}{V}. \tag{G16}$$

The *globally* self-consistent linearized osmotic pressure $\hat{P}^{\rm sgc}_{\rm DH}$, Eq. (G15), which preserves the exactness of the Legendre transformation, leads to results qualitatively similar to those of Eq. (70). In particular, the nonmonotonic behaviour of the spinodal lines for weak screening ($\kappa_{\rm b}a \ll 1$) and the intrinsic instability of the low-ϕ phase are still predicted by $\hat{P}^{\rm sgc}_{\rm DH}$, as shown in Figure 3, where we compare the spinodal lines associated with the two distinct semi-grand-canonical linearized osmotic-pressure definitions, given by Eqs. (70) and (G15). We should mention, however, that *explicit analytical* comparison in the exactly solvable planar case[27] does not show any improvement of the agreement between the nonlinear and linearized equations with the inclusion of the quadratic contribution to the average densities. Any *numerical* indications in this direction, which were indeed observed in the planar case,[27] are purely fortuitous. In fact, asymptotic expansions in the weak-coupling ($\ell_B \to 0$) and in the ideal-gas limit of both linearized osmotic pressures in the planar case, $P^{\rm sgc}_{\rm DH}$ and $\hat{P}^{\rm sgc}_{\rm DH}$, agree with the full nonlinear PB version up to the *same order*.

References

[1] R. J. Hunter, *Introduction to Modern Colloid Science* (Oxford University Press, Oxford, 1993).

[2] D. F. Evans and H. Wennerström, *The colloidal domain: where physics, chemistry, biology, and technology meet,* 2nd ed. (Wiley, New York, 1999).

[3] H. Lodish, A. Berk, S. L. Zipursky, P. Matsudaira, D. Baltimore, and J. Darnell, *Molecular Cell Biology,* 4th ed. (W. H. Freeman, New York, 2000).

[4] B. Alberts, A. Johnson, J. Lewis, M. Raff, K. Roberts, and P. Walter, *Molecular Biology of the Cell,* 4th ed. (Garland, New York, 2002).

[5] C. Holm and K. Kremer, *Polyelectrolytes in solution — recent computer simulations,* in *Proceedings of the Yamada Conference on Polyelectrolytes,* edited by I. Noda and E. Kokufuta (Yamada Science Foundation, Osaka, 1999) pp.27.

[6] C. Holm and K. Kremer, *Computer simulations of charged systems,* in *Proceedings of the NATO Advanced Study Institute on Electrostatic Effects in Soft Matter and Biophysics,* edited by C. Holm, P. Kékicheff, and R. Podgornik (Kluwer, Dordrecht, 2001) pp.117.

[7] H. L. Friedman and W. D. T. Dale, *Electrolyte solutions at equilibrium,* in *Statistical mechanics, Part A: Equilibrium techniques,* edited by B. J. Berne (New York, Plenum, 1977) chapt.3, pp.85.

[8] P. W. Debye and E. Hückel, Phys. Z. **24**, 185 (1923).

[9] T. L. Hill, *An Introduction to Statistical Thermodynamics* (Dover Publications, New York, 1986).

[10] D. A. McQuarrie, *Statistical Mechanics* (Harper-Collins, New York, 1976).

[11] M. E. Fisher and Y. Levin, Phys. Rev. Lett. **71**, 3826 (1993); Y. Levin and M. E. Fisher, Physica A **225**, 164 (1996).

[12] Y. Levin, M. C. Barbosa, and M. N. Tamashiro, Europhys. Lett. **41**, 123 (1998).

[13] M. N. Tamashiro, Y. Levin, and M. C. Barbosa, Physica A **258**, 341 (1998).

[14] L. Onsager, Chem. Rev. **13**, 73 (1933).

[15] Y. Levin, Rep. Prog. Phys. **65**, 1577 (2002).

[16] J. N. Israelachvili, *Intermolecular and Surface Forces,* 2nd ed. (Academic Press, London, 1992).

[17] S. A. Safran, *Statistical Thermodynamics of Surfaces, Interfaces and Membranes* (Addison-Wesley, Reading Mass., 1994).

[18] R. R. Netz and H. Orland, Eur. Phys. J. E **1**, 203 (2000).

[19] M. Deserno and C. Holm, *Cell model and Poisson-Boltzmann theory: a brief introduction,* in Ref. [6] pp.27.

[20] M. Fushiki, J. Chem. Phys. **97**, 6700 (1992).

[21] R. M. Fuoss, A. Katchalsky, and S. Lifson, Proc. Natl. Acad. Sci. U.S.A. **37**, 579 (1951).

[22] T. Alfrey, P. W. Berg, and H. Morawetz, J. Polym. Sci. **7**, 543 (1951).

[23] R. A. Marcus, J. Chem. Phys. **23**, 1057 (1955).

[24] S. Alexander, P. M. Chaikin, P. Grant, G. J. Morales, P. Pincus, and D. Hone, J. Chem. Phys. **80**, 5776 (1984).

[25] A. W. C. Lau and P. Pincus, Eur. Phys. J. B **10**, 175 (1999).

[26] S. H. Behrens and M. Borkovec, Phys. Rev. E **60**, 7040 (1999).

[27] M. N. Tamashiro and H. Schiessel, next following paper in this issue.

[28] C. A. Tracy and H. Widom, Physica A **244**, 402 (1997).

[29] D. Goulding and J.-P. Hansen, Europhys. Lett. **46**, 407 (1999).

[30] J. C. Neu, Phys. Rev. Lett. **82**, 1072 (1999); J. E. Sader and D. Y. C. Chan, J. Colloid Interface Sci. **213**, 268 (1999); *ibid.* **218**, 423 (1999); Langmuir **16**, 324 (2000); E. Trizac, Phys. Rev. E **62**, R1465 (2000).

[31] W. R. Bowen and A. O. Sharif, Nature (London) **393**, 663 (1998); *ibid.* **402**, 841 (1999).

[32] O. Spalla and L. Belloni, Phys. Rev. Lett. **74**, 2515 (1995); L. Belloni and O. Spalla, J. Chem. Phys. **107**, 465 (1997).

[33] Y. Levin, Physica A **265**, 432 (1999).

[34] B. V. Derjaguin and L. Landau, Acta Physicochimica (USSR) **14**, 633 (1941).

[35] E. J. W. Verwey and J. Th. G. Overbeek, *Theory of the Stability of Lyophobic Colloids* (Elsevier, Amsterdam, 1948).

[36] G. M. Kepler and S. Fraden, Phys. Rev. Lett. **73**, 356 (1994).

[37] M. D. Carbajal-Tinoco, F. Castro-Roman, and J. L. Arauz-Lara, Phys. Rev. E **53**, 3745 (1996).

[38] J. C. Crocker and D. G. Grier, Phys. Rev. Lett. **77**, 1897 (1996).

[39] A. E. Larsen and D. G. Grier, Phys. Rev. Lett. **76**, 3862 (1996); Nature (London) **385**, 230 (1997).

[40] D. G. Grier and J. C. Crocker, Phys. Rev. E **61**, 980 (2000).

[41] N. Ise, T. Okubo, M. Sugimura, K. Ito, and H. J. Nolte, J. Chem. Phys. **78**, 536 (1983); S. Dosho, N. Ise, K. Ito, S. Iwai, H. Kitano, H. Matsuoka, H. Nakamura, H. Okumura, T. Ono, I. S. Sogami, Y. Ueno, H. Yoshida, and T. Yoshiyama, Langmuir **9**, 394 (1993); N. Ise, T. Konishi, and B. V. R. Tata, *ibid.* **15** 4176 (1999).

[42] K. Ito, H. Hiroshi, and N. Ise, Science **263**, 66 (1994); B. V. R. Tata, E. Yamahara, P. V. Rajamani, and N. Ise, Phys. Rev. Lett. **78**, 2660 (1997).

[43] B. V. R. Tata, M. Rajalakshmi, and A. K. Arora, Phys. Rev. Lett. **69**, 3778 (1992).

[44] T. Palberg and M. Würth, Phys. Rev. Lett. **72**, 786 (1994).

[45] N. Grønbech-Jensen, K. M. Beardmore, and P. Pincus, Physica A **261**, 74 (1998).

[46] P. Linse and V. Lobaskin, Phys. Rev. Lett. **83**, 4208 (1999).

[47] E. Allahyarov and H. Löwen, Phys. Rev. E **63**, 041403 (2001).

[48] R. Messina, C. Holm, and K. Kremer, Phys. Rev. Lett. **85**, 872 (2000); Phys. Rev. E **64**, 021405 (2001).

[49] I. Sogami and N. Ise, J. Chem. Phys. **81**, 6320 (1984); M. V. Smalley, Mol. Phys. **71**, 1251 (1990); I. S. Sogami, T. Shinohara, and M. V. Smalley, *ibid.* **76**, 1 (1992); M. V. Smalley and I. S. Sogami, *ibid.* **85**, 869 (1995).

[50] B. Beresford-Smith, D. Y. C. Chan, and D. J. Mitchell, J. Colloid Interface Sci. **105**, 216 (1985).

[51] D. Y. C. Chan, Phys. Rev. E **63**, 061806 (2001).

[52] R. van Roij and J.-P. Hansen, Phys. Rev. Lett. **79**, 3082 (1997).

[53] R. van Roij, M. Dijkstra, and J.-P. Hansen, Phys. Rev. E **59**, 2010 (1999).

[54] J.-P. Hansen and H. Löwen, Annu. Rev. Phys. Chem. **51**, 209 (2000).

[55] P. B. Warren, J. Chem. Phys. **112**, 4683 (2000).

[56] A. R. Denton, Phys. Rev. E **62**, 3855 (2000).

[57] D. Y. C. Chan, P. Linse, and S. N. Petris, Langmuir **17**, 4202 (2001).

[58] S. N. Petris and D. Y. C. Chan, J. Chem. Phys. **116**, 8588 (2002).

[59] L. B. Bhuiyan and C. W. Outhwaite, J. Chem. Phys. **116**, 2650 (2002).

[60] J. Th. G. Overbeek, J. Chem. Phys. **87**, 4406 (1987); C. E. Woodward, *ibid.* **89**, 5140 (1988); J. Th. G. Overbeek, Mol. Phys. **80**, 685 (1993); Y. Rosenfeld, Phys. Rev. E **49**, 4425 (1994); D. G. Hall, Langmuir **12**, 4308 (1996); E. Trizac, *ibid.* **17**, 4793 (2001).

[61] K. S. Schmitz and L. B. Bhuiyan, Langmuir **18**, 1457 (2002); K. S. Schmitz, Phys. Rev. E **65**, 061402 (2002).

[62] P. Linse and V. Lobaskin, J. Chem. Phys. **112**, 3917 (2000); P. Linse, *ibid.* **113**, 4359 (2000); V. Lobaskin, A. Lyubartsev, and P. Linse, Phys. Rev. E **63**, 020401 (2001).

[63] A. Diehl, M. C. Barbosa, and Y. Levin, Europhys. Lett. **53**, 86 (2001).

[64] H. H. von Grünberg, R. van Roij, and G. Klein, Europhys. Lett. **55**, 580 (2001).

[65] M. Deserno and H. H. von Grünberg, Phys. Rev. E **66**, 011401 (2002).

[66] E. Trizac and J.-P. Hansen, Phys. Rev. E **56**, 3137 (1997).

[67] H. Löwen, J.-P. Hansen, and P. A. Madden, J. Chem. Phys. **98**, 3275 (1993).

[68] We should note that $\delta\beta U/\delta n(\boldsymbol{r}) = (\ell_B/2)\int \mathrm{d}^3\boldsymbol{r}'\,\mathrm{d}^3\boldsymbol{r}''\,\delta^3(\boldsymbol{r}'-\boldsymbol{r})\,G_3(\boldsymbol{r}',\boldsymbol{r}'')\,\rho(\boldsymbol{r}'') + (\ell_B/2)\int \mathrm{d}^3\boldsymbol{r}'\,\mathrm{d}^3\boldsymbol{r}''\,\rho(\boldsymbol{r}')\,G_3(\boldsymbol{r}',\boldsymbol{r}'')\,\delta^3(\boldsymbol{r}''-\boldsymbol{r}) = \psi(\boldsymbol{r})$.

[69] Rigorously one should take the total derivative with respect to the *total* WS-cell volume, $\tilde{V} \equiv 1/n_\mathrm{p} = V/(1-\phi)$. However, because we are assuming that the polyions are incompressible, $\mathrm{d}\tilde{V} = \mathrm{d}V$.

[70] H. Wennerström, B. Jönsson, and P. Linse, J. Chem. Phys. **76**, 4665 (1982).

[71] In the usual linearized-PB treatment of the spherical WS cell,[24] the gauge is chosen so that the electrostatic potential at the WS-cell boundary vanishes, $\psi(r = R) = 0$. The uniform counterion density, n_c, is then replaced by the counterion density at the WS-cell boundary, $n(R)$, and $\beta\mu_{el} = 0$, that is, $n(\boldsymbol{r}) = n(R)[1-\psi(\boldsymbol{r})]$. The normalization constant $n(R)$ is fixed by the charge-neutrality constraint (7), $n^{-1}(R) = \int \mathrm{d}^3\boldsymbol{r}\ [1 - \psi(\boldsymbol{r})]\,/Z$. This leads to an eigenvalue equation for κ, $2Z\kappa\ell_B = \Delta_2(\kappa R, \kappa a)$, where $\Delta_2(u, v)$ is defined by Eq. (28). This usual solution is, however, not *gauge invariant* (neither explicitly nor implicitly). For example, by choosing the gauge in which the potential $\psi(r = b)$ vanishes at an arbitrary distance $a \leq b \leq R$, one obtains the eigenvalue equation $Z\ell_B\Delta_1(\kappa R, \kappa b) = b\Delta_2(\kappa R, \kappa a)$ for κ, where $\Delta_1(u, v)$ is defined by Eq. (27). In other words, in the usual linearized-PB treatment the screening length κ^{-1} depends on the arbitrary distance b where the electrostatic potential is chosen to vanish and, therefore, the associated equations are clearly not gauge-invariant. This lack of gauge invariance just reflects the different choices for the expansion densities, which are allowed in this approach. We should also remark that this linearization procedure — associated with the definition of a renormalized charge — is based on an attempt to describe the asymptotic behaviour of the electrostatic potential in the vicinity of the WS-cell boundary — being thus a *local* approach to the linearization — while in the gauge-invariant scheme presented in the main text the linearization is based on a *global* description of the system, at the level of the whole free energy of the WS cell.

[72] We should stress that the electrostatic correction given by Eq. (32) was obtained by a linearization of the PB WS-cell functional, that takes only *intracell* polyion-microion correlations (at the mean-field level) into account. Therefore, it does not include any (neither inter- nor intracell) microion-microion correlations or *intercell* polyion-microion and polyion-polyion correlations. In the case of the (symmetric) RPM, where the mean-field contribution vanishes and only the microion-microion correlations are present, these lead to the famous Debye-Hückel electrostatic osmotic-pressure limiting law,[15] $-\kappa^3/(24\pi)$.

[73] M. O. Robbins, K. Kremer, and G. S. Grest, J. Chem. Phys. **88**, 3286 (1988).

[74] X.-J. Li, Y. Levin, and M. E. Fisher, Europhys. Lett. **26**, 683 (1994); M. E. Fisher, Y. Levin, and X.-J. Li, J. Chem. Phys. **101**, 2273 (1994).

[75] M. Medina-Noyola and D. A. McQuarrie, J. Chem. Phys. **73**, 6279 (1980).

[76] Y. Levin, private communication. The resemblance between the asymptotic excess free energy (47) when one subtracts out the polyion electrostatic self-energy, $Z^2\ell_B/(2a)$, and the *excess chemical potential* (or activity coefficient γ) of an ion inside a symmetric monovalent electrolyte in the traditional DH theory, cf. Eq. (15-74) of Ref. [10], is purely fortuitous.

[77] E. Güntelberg, Z. Phys. Chem. Stoechiom. Verwandtschaftsl. **123**, 199 (1926).

[78] L. Belloni, Colloid Surf. A **140**, 227 (1998).

[79] E. Trizac, L. Bocquet, and M. Aubouy, cond-mat/0201510; L. Bocquet, E. Trizac, and M. Aubouy, cond-mat/0210195.

[80] M. J. Stevens, M. L. Falk, and M. O. Robbins, J. Chem. Phys. **104**, 5209 (1996).

[81] M. N. Tamashiro and H. Schiessel. *Rayleigh instability of spherical charged droplets in the presence of added salt*. In preparation.

[82] G. Téllez and E. Trizac, cond-mat/0209114.

[83] F. G. Donnan, Chem. Rev. **1**, 73 (1924).

[84] J. Th. G. Overbeek, Prog. Biophys. Biophys. Chem. **6**, 57 (1956).

[85] T. L. Hill, Disc. Faraday Soc. **21**, 31 (1956); J. Phys. Chem. **61**, 548 (1957).

[86] V. Reus, L. Belloni, T. Zemb, N. Lutterbach, and H. Versmold, J. Phys. II France **7**, 603 (1997).

[87] M. N. Tamashiro, Y. Levin, and M. C. Barbosa, Eur. Phys. J. B **1**, 337 (1998).

[88] Note that the nonlinear osmotic-pressure difference satisfies $\beta\Delta P \equiv n_+(R) + n_-(R) - 2n_\mathrm{b} = 4n_\mathrm{b}\sinh^2\left\{\frac{1}{2}\left[\beta\mu_\mathrm{el} - \psi(R)\right]\right\} > 0$.

[89] *Handbook of Mathematical Functions,* edited by M. Abramowitz and I. A. Stegun (Dover, New York, 1970).

[90] This equivalence does not hold *beyond* the mean-level, because microionic correlations in the bulk salt reservoir will lead to different osmotic pressures in the two distinct cases.

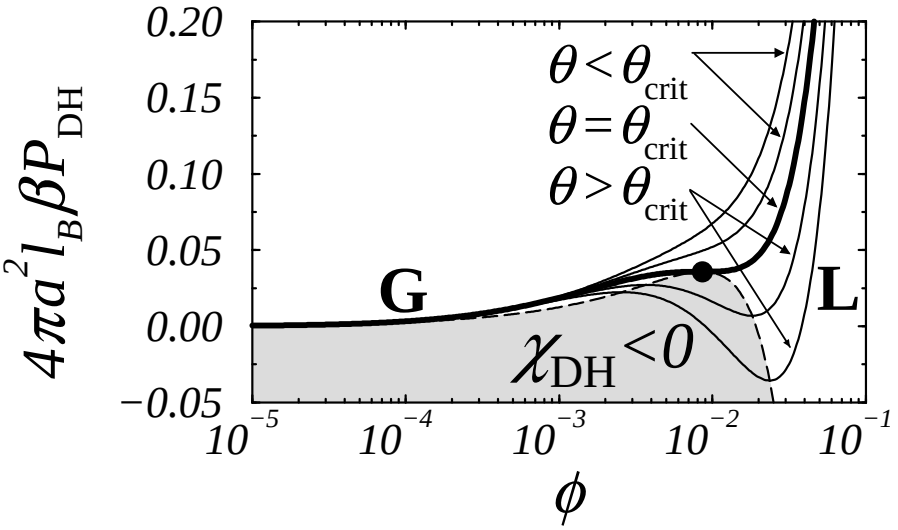


Figure 1: Salt-free ($s = 0$) linearized osmotic-pressure isotherms as a function of the volume fraction $\phi = (a/R)^3$. From top to bottom the isotherms correspond to $\theta = 41, 43, \theta_{\rm crit} = 44.902477\cdots$ (bold line), 47 and 49. In the gray region the salt-free linearized isothermal compressibility $\chi_{\rm DH}$ is negative, which would imply a thermodynamical instability that leads to a phase separation between two fluid phases: a low-ϕ (dilute) gas (G) and a high-ϕ (dense) liquid (L). The black circle represents the salt-free critical osmotic pressure and the dashed curve defines the salt-free spinodal line in the $\theta \times \phi$ diagram (the $s = 0$ line in Figure 2).

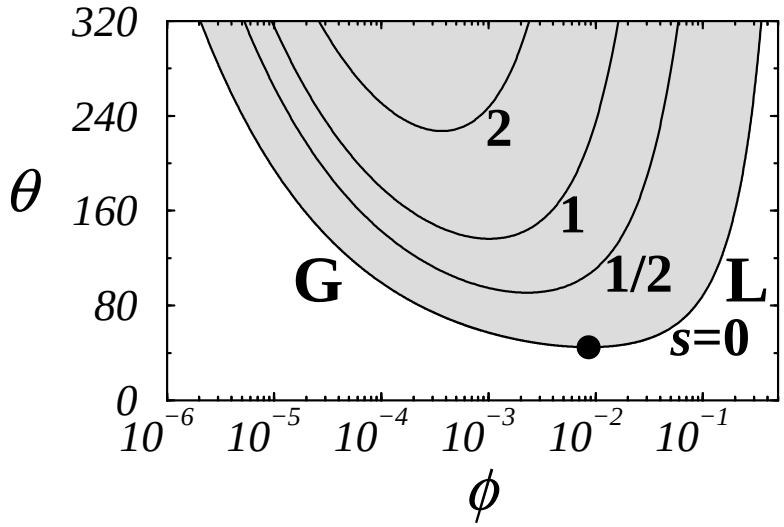


Figure 2: Spinodal lines associated with the linearized canonical osmotic pressure $P_{\rm DH}^{\rm can}$, in the $\theta = 3Z\ell_B/a$ versus volume fraction $\phi = (a/R)^3$ plane. They correspond to lines of vanishing inverse isothermal compressibility, $\chi_{\rm DH}^{-1} = 0$. In the gray region the linearized isothermal compressibility of the salt-free ($s = 0$) suspension becomes negative, leading to a coexistence between gas (G) and liquid (L) fluid phases. Note that this is in contrast to the full nonlinear treatment,[82] which *always* predicts positive compressibilities. Addition of monovalent salt reduces the unstable region by shifting the spinodal lines to higher values of θ, as labeled by the different curves with increasing values of s. The black circle represents the salt-free critical point (see main text for more details).

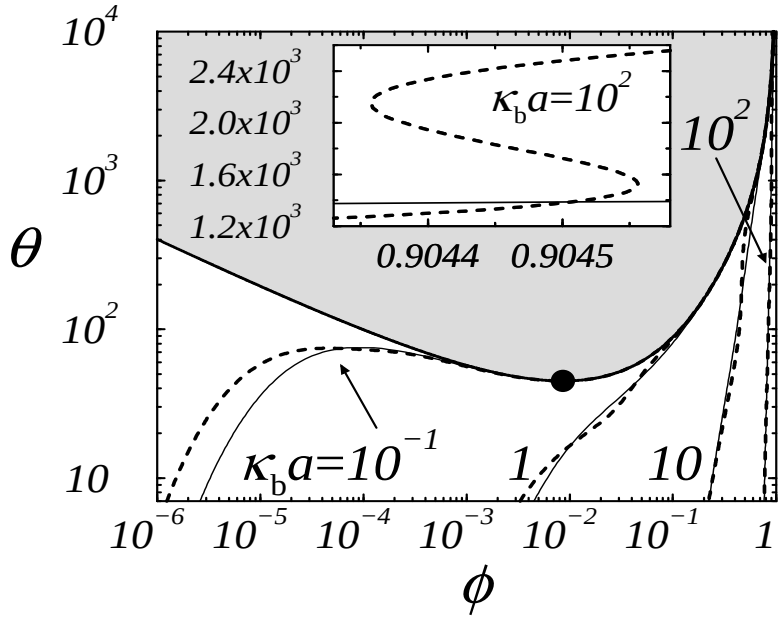


Figure 3: Spinodal lines ($\chi_{\rm DH}^{-1} = 0$) associated with the linearized semi-grand-canonical osmotic pressures $P_{\rm DH}^{\rm sgc}$ (dashed lines), Eq. (70), and $\hat{P}_{\rm DH}^{\rm sgc}$ (solid lines), Eq. (G15), in the $\theta = 3Z\ell_B/a$ versus volume fraction $\phi = (a/R)^3$ plane. They delimit the spurious unstable region that extends to lower values of ϕ. To allow a comparison with the canonical case (Figure 2), we also show the salt-free critical point (black circle) and the salt-free ($\kappa_{\rm b}a = 0$) unstable gray region. In the salt-free limit ($\kappa_{\rm b}a \ll 1$) the semi-grand-canonical spinodal line reduces to the salt-free one, although for any nonvanishing $\kappa_{\rm b}a$ eventually it will bend to the zero-temperature critical point at $(\phi_{\rm crit}, \theta_{\rm crit}) = (0, 0)$. Contrary to the canonical case, an increase of the bulk reservoir density in the semi-grand-canonical case *enhances the instability,* as can be seen from the different spinodal lines with increasing $\kappa_{\rm b}a$. A typical monotonic (non-oscillating) osmotic-pressure isotherm is presented in Figure 3 (dotted curve) in Ref. [65]. See also main text for additional comments.